USAFTPS-TIM-20A-03

POSITION CORRECTIONS AND STALL CHARACTERISTICS OF EPIC MODIFIED C-12C

(Project Have EPIC DISCO)

JOHN STEVENSON, Capt, USAF
Project Manager/WSO

SARAH VORGERT, Capt, USAF
Project Engineer

ERIC HICKERNELL, Maj, USAF
Project Pilot

DOUG WEIDMAN, Capt, USAF
Project Pilot

W. TRAVIS JOHNSON, LT, USN
Project Pilot

RACHEL WILLIAMS, Capt USAF
Project Pilot

DECEMBER 2020

FINAL TECHNICAL INFORMATION MEMORANDUM

USAF TPS

UNITED STATES AIR FORCE TEST PILOT SCHOOL
AIR FORCE TEST CENTER
EDWARDS AIR FORCE BASE, CALIFORNIA
AIR FORCE MATERIEL COMMAND
UNITED STATES AIR FORCE

This technical information memorandum (USAFTPS-TIM-20A-03, *Position Corrections and Stall Characterization of EPIC Modified C-12C*) was submitted under job order number MT20A300 by the Commandant, USAF Test Pilot School, Edwards AFB, California 93524-6843.

Prepared by:

STEVENSON.JOHN.ARIS.1460089103 Digitally signed by STEVENSON.JOHN.ARIS.1460089103 Date: 2020.12.08 08:53:34 -08'00'

JOHN A. STEVENSON
Captain, USAF
Project Manager/WSO

VORGERT.SARAH.ANN.1405248111 Digitally signed by VORGERT.SARAH.ANN.1405248111 Date: 2020.12.08 10:17:20 -08'00'

SARAH A. VORGERT
Captain, USAF
Project Engineer

HICKERNELL.ERIC.L.1297100986 Digitally signed by HICKERNELL.ERIC.L.1297100986 Date: 2020.12.08 10:36:11 -08'00'

ERIC L. HICKERNELL
Major, USAF
Project Pilot

WEIDMAN.DOUGLAS.J.1300924014 Digitally signed by WEIDMAN.DOUGLAS.J.1300924014 Date: 2020.12.08 10:47:34 -08'00'

DOUG J. WEIDMAN
Captain, USAF
Project Pilot

JOHNSON.WILLIAM.TRAVIS.III.1284096858 Digitally signed by JOHNSON.WILLIAM.TRAVIS.III.1284096858 Date: 2020.12.08 10:18:35 -08'00'

W. TRAVIS JOHNSON
Lieutenant, USN
Project Pilot

WILLIAMS.RACHEL.W.1388065920 Digitally signed by WILLIAMS.RACHEL.W.1388065920 Date: 2020.12.08 08:52:35 -08'00'

RACHEL W. WILLIAMS
Captain, USAF
Project Pilot

This test plan has been reviewed and is approved for publication:

JURADO.JUAN.D.1272700300 Digitally signed by JURADO.JUAN.D.1272700300 Date: 2020.12.08 13:43:03 -08'00'

JUAN D. JURADO, PhD
Lieutenant Colonel, USAF
Project Staff Advisor
USAF Test Pilot School

Digitally signed by MAJOR.KARL.B.1145510437 Date: 2020.12.08 12:17:27 -08'00'

KARL B. MAJOR
NH-04, DAF
Project Staff Advisor
USAF Test Pilot School

Digitally signed by LEE.CHIAWEI.NMN.1300514088 Date: 2020.12.08 11:58:09 -08'00'

CHIAWEI N. LEE
NH-03, DAF
Test Management Program Director
USAF Test Pilot School

VANHOY.DAVID.L.1229799688 Digitally signed by VANHOY.DAVID.L.1229799688 Date: 2021.02.01 15:49:43 -08'00'

DAVD L. VANHOY
NH-04, DAF
Technical Director
USAF Test Pilot School

PABON.SEBRINA.L.1015514848 Digitally signed by PABON.SEBRINA.L.1015514848 Date: 2021.02.01 16:07:12 -08'00'

SEBRINA L. PABON
Colonel, USAF
Commandant
USAF Test Pilot School

REPORT DOCUMENTATION PAGE

Form Approved
OMB No. 0704-0188

1. REPORT DATE *(DD-MM-YYYY)*	2. REPORT TYPE	3. DATES COVERED *(From - Through)*
07-12-2020	Final Technical Information	01 SEPT - 24 SEPT 2020

4. TITLE AND SUBTITLE

Position Corrections and Stall Characteristics of EPIC Modified C-12C

5A. CONTRACT NUMBER

5B. GRANT NUMBER

5C. PROGRAM ELEMENT NUMBER

6. AUTHOR(S)

JOHN STEVENSON, Capt, USAF
Project Manager/WSO

SARAH VORGERT, Capt, USAF
Project Engineer

ERIC HICKERNELL, Maj, USAF
Project Pilot

DOUG WEIDMAN, Capt, USAF
Project Pilot

W. TRAVIS JOHNSON, LT, USN
Project Pilot

RACHEL WILLIAMS, Capt USAF
Project Pilot

5D. PROJECT NUMBER
MT20A300

5E. TASK NUMBER

5F. WORK UNIT NUMBER

7. PERFORMING ORGANIZATION NAME(S) AND ADDRESS(ES)
Air Force Test Center
412th Test Wing
USAF Test Pilot School
Edwards AFB CA 93524-6485

8. PERFORMING ORGANIZATION REPORT NUMBER
USAFTPS-TIM-20A-03

9. SPONSORING / MONITORING AGENCY NAME(S) AND ADDRESS(ES)
USAF Test Pilot School
220 Wolfe Ave
Edwards AFB, California 93524-6843

10. SPONSOR/MONITOR'S ACRONYM(S)

11. SPONSOR/MONITOR'S REPORT NUMBER(S)

12. DISTRIBUTION / AVAILABILITY STATEMENT
See disclaimer on cover.

13. SUPPLEMENTARY NOTES
SC: 012100 CA: 412th Test Wing Edwards AFB CA Print this document in COLOR.

14. ABSTRACT

This report documents results of the C-12C EPIC-modified aircraft. Testing was requested by the USAF Test Pilot School, Edwards AFB, California. The lead developmental test organization was the Air Force Test Center, Edwards AFB, California. The executing test organization was Class 20A of the USAF Test Pilot School, Edwards AFB. Testing was conducted from 01 to 24 September 2020 and comprised of 4.8 ground test hours and 14 sorties totaling 21.2 flight test hours. The overall test objective was to determine the flight idle stall speeds and the effects of AOA and Mach on static position error of the C-12C EPIC-modified aircraft. All test objectives were met.

15. SUBJECT TERMS
C-12C stall speeds, SPE (Static Position Error), AOA (Angle of Attack), Mach, JMOSS (Jurado-McGehee Online Self-Survey Method), EPIC (Enhanced Performance Increased Capability)

16. SECURITY CLASSIFICATION OF:			17. LIMITATION OF ABSTRACT	18. NUMBER OF PAGES	19A. NAME OF RESPONSIBLE PERSON
a. REPORT	b. ABSTRACT	c. THIS PAGE			Karl Major
U	U	U	Same as Report	73	19B. TELEPHONE NUMBER (INCLUDE AREA CODE) 661-277-8892

This page was intentionally left blank.

EXECUTIVE SUMMARY

This report presents the results of the position corrections and stall characteristics of the Enhanced Performance Increased Capability (EPIC) modified C-12C under the project name Have EPIC DISCO. Testing was requested by the United States Air Force (USAF) Test Pilot School (TPS), and the lead developmental test organization was the Air Force Test Center, Edwards AFB, California. The executing test organization was USAF TPS Class 20A, Edwards AFB. Testing was conducted at Edwards AFB from 01 to 24 September 2020 and comprised of 4.8 ground test hours and 14 sorties totaling 21.2 flight test hours.

In 2015, the C-12C fleet was modified with the EPIC Platinum Performance Package, which included the addition of swept blade turbofan propellers and modification of the inboard leading edges. The published stall data for the modified C-12C showed lower stall speeds than unmodified C-12C. Initial flight tests to determine the new stall speeds of modified C-12C used a zero-thrust power setting instead of the flight idle setting specified by the American Society for Testing and Materials Standard F3179, which was used for FAA certification. Since the C-12C had more drag in flight idle compared to the zero thrust power setting, the published stall data in the flight manual was not the most conservative. Higher stall speeds at idle thrust could have affected calculation of safe maneuvering, takeoff, and landing speeds.

Static Position Error (SPE), which is used in air data system calibration, had traditionally been determined using the tower flyby, survey, or pacer methods, which each required additional calibrated assets or infrastructure that may not be available for a program. Tower flyby and pacer were also generally limited to steady-state conditions, which restricted the data collection capabilities at very slow airspeeds, such as near the stall speed of the aircraft. For this reason, tower flyby and pacer methods required extrapolation to determine SPE at stall speeds. To calculate SPE directly, the staff at Test Pilot School had been independently investigating the use of a quasi-steady flight test technique; the Jurado-McGehee Online Self Survey (JMOSS) method. This project applied the JMOSS method across different weights and pressure altitudes to calculate SPE and to model the individual contributions of Mach and angle of attack.

This program had two general test objectives. The first was to determine the stall speeds of an EPIC-modified C-12C and the second was to determine the independent effects of Angle of Attack (AOA) and Mach number on static position error.

A C-12C equipped with Data Acquisition System (DAS) and a nose boom was used for the majority of the test program. Stalls were accomplished at idle power with wings level in flaps up and gear up, flaps 40% and gear down, and flaps 100% and gear down configurations. Aircraft gross weight was between 10,550 and 12,250 pounds and aircraft center of gravity was held between 0 and 20 % of the forward limit. Testing occurred between 8,000 and 20,000 feet pressure altitude. Stall speeds in all configurations were spot checked in a non-DAS, fleet representative C-12C.

Overall, both objectives were met. The wings level stall speeds of EPIC-modified C-12C were as much as seven knots higher than the stall speeds currently published in the aircraft flight manual. Stall testing in the fleet representative C-12C also revealed few statistically significant differences between the stall speeds of DAS and non-DAS aircraft, with all stall speeds higher than EPIC numbers. This meant that the flight test boom did not significantly alter the stall speed and that the collected DAS stall speeds could be considered fleet-representative. Additionally, the JMOSS method successfully determined the static position error of the C-12C and revealed the relationship of static position error to Mach and angle of attack. Although both variables exhibited a statistically significant relationship, AOA was not found to have a strong effect on the SPE variance and was not a good predictor of SPE in the C-12C. The test team recommends that the stall speeds in the C-12C flight manual should be updated to reflect the higher stall speeds discovered during this test program.

This page was intentionally left blank.

TABLE OF CONTENTS

This page was intentionally left blank

INTRODUCTION

This report presents the results of the position corrections and stall characteristics of the Enhanced Performance Increased Capability (EPIC) modified C-12C under the project name Have EPIC DISCO. Testing was requested by the United States Air Force (USAF) Test Pilot School (TPS), and the lead developmental test organization was the Air Force Test Center, Edwards AFB, California. The executing test organization was USAF TPS Class 20A, Edwards AFB. Testing was conducted at Edwards AFB from 01 to 24 September 2020 and comprised of 4.8 ground test hours and 14 sorties totaling 21.2 flight test hours.

BACKGROUND

Air data system position corrections were required to calculate calibrated stall speed. This project employed a quasi-steady method to directly calculate Static Position Error (SPE) at a wide range of airspeeds to include stall speed. This method also gathered data to determine possible predictor factors for SPE. Stall speeds and SPE predictor factors were determined using the same platform and a combined flight test technique (FTT). Testing was conducted by the Have EPIC DISCO Test Team in accordance with the test plan, *Position Corrections and Stall Characteristics of EPIC Modified C-12C* (reference 1).

Determination of Stall Speeds

Aircraft stall speeds were defined in MIL-STD-1797B (reference 2) as the highest of the speed for steady straight flight at C_{Lmax}, the speed at which uncommanded pitching, rolling, or yawing occurs, or the speed at which intolerable buffet or structural vibration are encountered. The Federal Aviation Administration (FAA) defined stall speeds in American Society for Testing and Materials (ASTM) Compliance Standard F3180, paragraph 4.2.2.2 (reference 3). The FAA Advisory Circular 23-8C (reference 4) provided further guidance on both stall conditions and test procedures, defining stall as the first of the following conditions to occur: “uncontrollable downward pitching motion”, “downward pitching motion resulting from the activation of a device (for example, stick pusher)” or, “the control reaches the stop”. Based on ASTM Compliance Standard F3179, paragraph 5.1.1 (reference 5), for turboprop engine aircraft, stall testing should be conducted at “the propulsive thrust not greater than zero at the stalling speed, or, if the resultant thrust has no appreciable effect on the stalling speed, with engine(s) idling and throttle(s) closed”. The Circular clarified this statement saying stall speed should be obtained at either flight idle (defined as “propellers in the takeoff position and the engines idling with throttles closed”) or at zero thrust (defined as “sufficient power to produce zero propeller thrust”) “if idle thrust has no appreciable effect on stall speed,” whichever is more conservative. For the C-12C, zero thrust was at a higher engine setting than flight idle, which made flight idle the more conservative setting. Preliminary test results from the Pirate Snail Pacer test program indicated that the C-12C was predicted to exhibit stall characteristics of a downward pitching motion, with a slight potential for the yoke reaching the full aft position when the flaps were set to 40 percent (reference 6).

The C-12 fleet was modified with the EPIC Platinum Performance Package in 2015. This modification was installed on all four C-12C aircraft operated by USAF TPS, tail numbers 73-1215, 76-0158, 76-0161 and 76-0166. These modifications altered the stall speed of the aircraft and new stall speeds were published in the T.O. 1C-12A-1 Flight Manual (reference 7).

The Defense Security Cooperation Agency (DSCA) noted small stall speed discrepancies from the published speeds on the first C-12s to be modified with the EPIC package. USAF TPS started to collect

informal data on this discrepancy as Edwards Air Force Base received their first modified aircraft in winter of 2015. On 11 July 2016, the C-12 Program Office was notified of an issue relating to significantly higher than expected stall speeds on aircraft at Edwards AFB. The stall speed observed was approximately equal to the charted takeoff rotation speed, which was well below the 10% safety margin accepted by the industry as stated in ASTM Standard F3179 (reference 5). The Program Office acknowledged an issue in the initial buffet ranges published in 1C-12A-6CF-1 (reference 8) for an 11,300 lb aircraft in the Gear and Flaps Down and Gear and Flaps Up configurations. The Program Office updated the functional check flight procedures checklist (1C-12A-6CF-1) to correct the initial buffet ranges. However, the Program Office did not address the stall speed discrepancy but authorized Edwards AFB to use the non-EPIC (T.O. 1C-12A-1) takeoff performance data to compensate conservatively for any possible stall speed discrepancies (reference 9).

On 7 September 2016, flight idle stall speeds were informally recorded on EPIC aircraft 73-1215 during a routine flight at USAF TPS. Recorded stall speeds were observed up to 8.5 knots higher than the stall speed in the flight manual. Additional stall data from similar sorties conducted from 4 to 28 August 2016 on aircraft 73-1215 indicated stall speeds up to 8.5 knots higher than the flight manual.

A representative from the EPIC certification effort indicated that the stall speeds for the EPIC modification Supplemental Type Certificate (and Flight Manual) were determined using the zero thrust approach, while stalls performed at USAF TPS were conducted using the flight idle approach, which possibly accounted for the observed difference. Flight idle power settings created negative thrust, which reduced airflow over the inboard portion of the wings and resulted in a worse stall condition at higher airspeeds than at zero thrust. TPS began investigating the difference between zero thrust and flight idle stall speeds on the C-12C with the Pirate Snail Pacer test program (reference 10). This test program was never completed, but preliminary results confirmed a difference between the two airspeeds. Since the observed flight idle stall speeds appeared consistently higher or more conservative than the stall speeds published in the flight manual, systematic rigorous testing was warranted to determine the actual flight idle stall speeds. This systemic test approach was one objective of this test program.

Determination of Position Correction Predictors

Independent of the C-12C EPIC modification stall speeds, USAF TPS had been investigating the use of a quasi-steady flight test technique to determine the SPE of an aircraft in flight. The SPE had traditionally been determined using the tower flyby, survey, or pacer methods, which each required additional calibrated assets or infrastructure that may not be available for a program. Tower flyby and pacer were also generally limited to steady-state conditions, which restricted the data collection capabilities at very slow airspeeds, such as near the stall speed of the aircraft. For this reason, tower flyby and pacer methods required extrapolation to determine SPE at stall speeds. The quasi-steady FTT, called the Jurado-McGehee Online Self Survey (JMOSS) method (reference 11) could determine SPE accurately and directly without additional assets, and at speeds down to stall.

Previous testing in the Have SPEED test program (reference 12) demonstrated the validity of the JMOSS method to cover a wide range of Mach numbers in a quasi-steady FTT consisting of a level deceleration with a minimum 360-degree constant airspeed turn. This method was able to determine the SPE by comparing the Pitot-static measured airspeed to the true airspeed calculated by the Global Positioning System (GPS) ground speed and winds aloft, which were estimated from the constant airspeed turn. The JMOSS algorithm also estimated a temperature recovery factor (K_t), making the algorithm self-contained. The SPE calculation required the assumption that the Pitot-static measured airspeed error was only due to SPE (total pressure error was negligible) and that the winds were constant throughout the

maneuver. JMOSS estimated ambient pressure using the difference between GPS airspeed and air data system indicated airspeed. It could also include ambient pressure and ambient temperature measured from a weather balloon as an optional input.

After initial validation in the Have SPEED program, the JMOSS method was used to determine the SPE for a C-130 in May 2018 (reference 13). The results close to ground level closely matched the SPE calculated by the Tower Flyby FTT, while the JMOSS tests done at altitude followed a different SPE curve. This indicated that as the relationship between Mach and angle of attack (AOA) changed due to the ratio of aircraft gross weight (W) to the altitude-based pressure (δ) ratio (W/δ), the SPE curves also changed. However, the test did not employ weather balloons to validate the SPE curves. Additionally, the weight state of the airplane was not properly recorded. In order to properly characterize these SPE relationships, the second objective for this test plan was to determine the individual contributions of Mach and AOA on SPE.

In order to determine the individual effects of Mach and AOA on SPE, large changes in W/δ were necessary. These effects were not seen in Have SPEED's testing on a T-38, but were observed in testing involving a C-130. Without access to a C-130-size aircraft or larger to create weight changes, the C-12C was used as a light cargo platform to measure the Mach and AOA effects on SPE.

TEST ITEM DESCRIPTION

The systems under test were two C-12C aircraft with the EPIC Platinum performance modifications. The two aircraft used for testing were tail numbers 76-0158 and 76-0166. Tail number 76-0158 was a Data Acquisition System (DAS) equipped aircraft instrumented with a flight test nose boom, shown in Figure 1. Tail number 76-0166 was a non-DAS aircraft, representative of a standard C-12C fleet aircraft. The EPIC modifications included a ram air recovery system (RARS), dual aft body strakes, high flotation gear doors, swept blade turbofan propellers, and enhanced performance inboard leading edges. Each modification was intended to improve the aircraft performance of the C-12C.

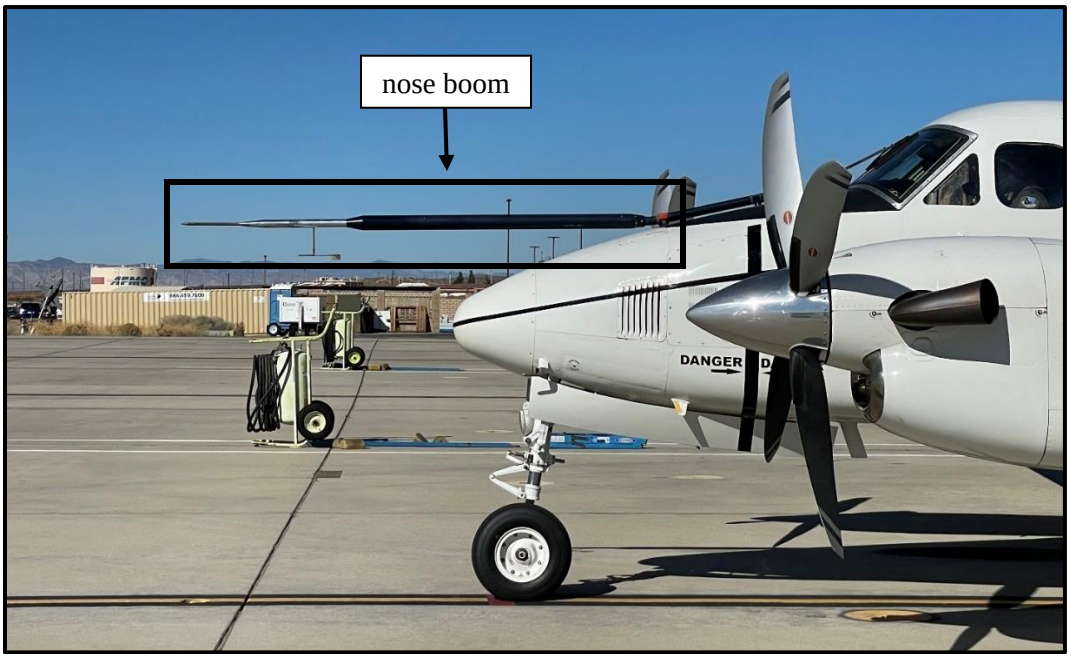

Figure 1. Flight test nose boom

The RARS, shown in Figure 2, was designed to improve climb and cruise performance and to improve engine efficiency by lowering Turbine Gas Temperature (TGT) and thus increasing available horsepower when the engines were temperature limited, but not torque limited. The RARS modification also was intended to reduce the aerodynamic penalty for deploying the ice vanes as ice vane deployment raised TGT.

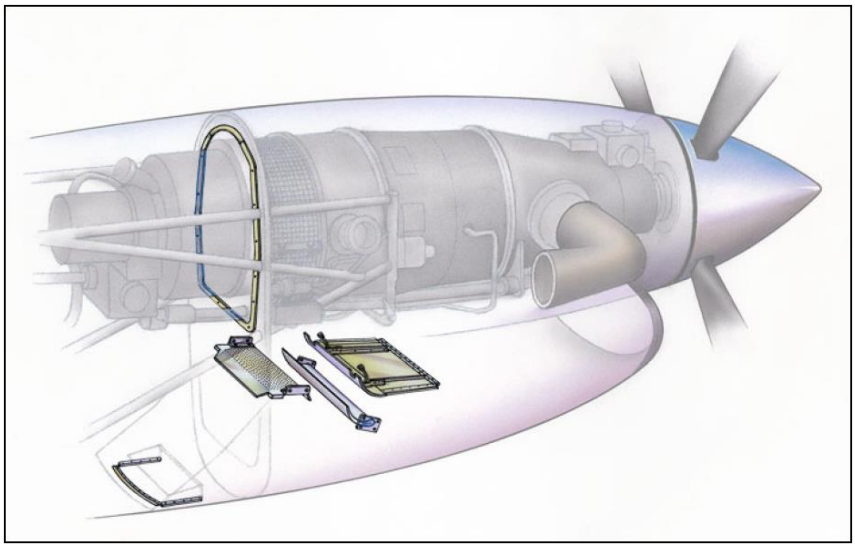

Figure 2. Ram Air Recovery System

The dual aft body strakes, as seen in Figure 3, were designed to increase climb and cruise performance, enhance handling qualities, and eliminate the yaw damper requirement above 17,000 ft.

Figure 3. Dual Aft Body Strakes

Figure 4 shows the high flotation gear doors. These gear doors were designed to minimize drag by fully enclosing the landing gear.

Figure 4. High Flotation Gear Doors

Figure 5 shows the swept-blade turbofan propellers, which were designed to increase low-speed acceleration and improve takeoff and landing performance.

Figure 5. Swept Blade Turbofan Propellers

The inboard wing leading edge modification changed the airfoil shape, and was designed to increase cruise speeds and range. The new leading edges were also designed to reduce airflow separation inboard of the engine, intending to create a more elliptical lift distribution across the entire wing. Figure 6 shows the approximate lift profiles for the basic aircraft on the left and the EPIC modification on the right.

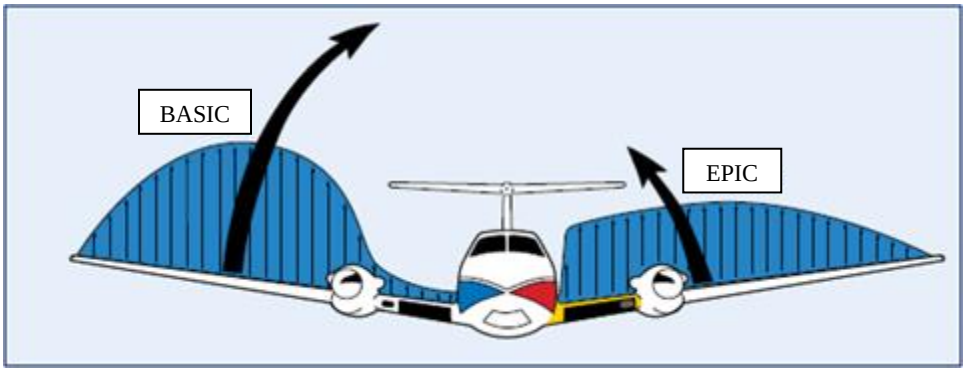

Figure 6. Inboard Wing Leading Edge Lift Distribution

According to the flight manual (reference 7), the Pitot-static system provided a source of impact air and static air for the Air Data Computers (ADC 1 and ADC 2). A Pitot probe was located on each side of the lower portion of the nose. Additionally, the DAS aircraft was equipped with a flight test nose boom, which provided yaw angle (sideslip), angle of attack, and Pitot and static pressure to the DAS. Static pressure from the boom was not considered accurate and was not used. The air data system is a dual Air Data Computer (ADC) system that senses and processes data derived from the air mass around the aircraft. The airspeed tape on the primary flight displays (PFD) indicated airspeed. Tubing connected each probe to the associated computers in the nose avionics bay. Information from the left Pitot probe was provided to ADC 1. There were four normal static ports located on the rear fuselage aft of the rear pressure bulkhead, two on each side. The four normal static ports provided two separate sources of static air, one for the pilot's system and one for the copilot's. Each of the normal static air system lines opened to the atmosphere through two static air ports, one on each side of the fuselage. The pilot's side received static information from the upper left and lower right ports and provided this information to ADC 1. The copilot's side received static information from the upper right and lower left ports and provided this information to ADC 2. There were three drain petcocks located on the right lower sidewall used for draining the static air lines. These drain valves were opened by maintenance to release any trapped moisture during routine scheduled inspections.

A GPS Aided Inertial Navigation Reference (GAINR) Lite rack was installed in the rear cargo compartment of the DAS C-12C to provide accurate time space position information (TSPI) for SPE calculations.

The aircraft was equipped with conventional dual controls for the pilot and copilot. The ailerons and elevators were operated by conventional control wheels interconnected by a T-column. The rudder pedals were interconnected by a linkage below the floor. These systems were connected to the control surfaces through closed cable-bellcrank systems. Rudder, elevator, and aileron trim were adjustable with controls mounted on the center pedestal. Position indicators for each of the trim tabs were integrated with their respective controls (reference 7). Yoke aft was considered a positive control deflection, which raised the trailing edge of the elevator. Trailing edge up was a negative surface deflection and resulted in a nose up pitching moment.

TEST OBJECTIVES

The first general test objective was to determine the stall speeds of C-12C EPIC aircraft at flight idle thrust conditions. The specific test objectives were to determine the flight idle stall speeds in cruise (Flaps Up, Gear Up), approach (Flaps 40%, Gear Down), and landing (Flaps 100%, Gear Down) configurations and to compare a sample of C-12C flight idle stall speeds between non-DAS and DAS EPIC-configured aircraft.

The second general test objective was to determine the static position error as a function of angle of attack and Mach number. The specific test objectives were to determine the statistical significance of angle of attack, Mach number, and the interaction of angle of attack and Mach number on static position error.

The general test objectives were met.

This page was intentionally left blank

TEST AND EVALUATION

Overall, the C-12C EPIC-modified aircraft flight idle stall speeds and static position error were successfully determined, resulting in defensible recommendations for flight manual updates. The wings level stall speeds of EPIC-modified C-12C aircraft were as much as seven knots higher than the stall speeds currently published in the aircraft flight manual. Stall testing in the fleet representative C-12C also revealed few statistically significant differences between the stall speeds of DAS and non-DAS aircraft, with all stall speeds higher than EPIC numbers. This meant that the flight test boom did not significantly alter the stall speed and that the collected DAS stall speeds could be considered fleet-representative. Additionally, the JMOSS method successfully determined the static position error of the C-12C and revealed the relationship of static position error to Mach and angle of attack. Although both variables exhibited a statistically significant relationship, AOA was not found to have a strong effect on the SPE variance and was not a good predictor of SPE in the C-12C. **Update C-12C flight manual stall speed figures to reflect the higher stall speeds determined during this program. (R1)**[1]

A C-12C equipped with DAS, a flight test nose boom, and a GAINR Lite rack was used for the majority of the test program objectives. Stalls were accomplished at idle power with wings level in clean, flaps 40% and gear down, and flaps 100% and gear down configurations. The "Angry Silv" FTT was used to calculate SPE and analyze SPE predictors from maximum level speed to stall speed. Aircraft gross weight was between 10,550 and 12,250 pounds and aircraft center of gravity was held between 0 and 20% of the forward limit. Stall testing and "Angry Silv" maneuvers occurred at three target pressure altitudes of 8,500 ft, 14,000 ft, and 19,500 ft in order to maximize the AOA variation for the SPE modeling. Additional SPE testing included tower fly-by passes targeting 200 feet AGL at target airspeeds of 140 KIAS, 180 KIAS and 240 KIAS. Stall speeds in all three configurations were spot checked at approximately 8,500 feet pressure altitude in a non-DAS, fleet representative C-12C.

OVERALL TEST METHODS AND CONDITIONS

Ground Calibration

The test team determined the instrument corrections of the air data systems of the two test aircraft on the ground using a known, calibrated pressure source applied to the pressure ports on the outside of the aircraft. The pressure sources simulated the air pressures at the test altitudes in 10-knot increments around stall speeds. The difference between the "truth" altitude/airspeed and the indicated altitude/airspeed was recorded and used as an instrument correction. This calibration was done on both the production (ADC 1) and DAS air data systems of the DAS aircraft and the pilot side production air data system (ADC 1) for the non-DAS aircraft. The details of the ground calibration process and the resultant instrument corrections for airspeed and altitude on both aircraft are described in detail in Appendix A. The ground calibration data were not employed in the DAS aircraft speed calculations, but were used for the non-DAS aircraft.

The "Angry Silv"

The "Angry Silv" FTT combined several maneuvers in order to explore the relationship between AOA, Mach, and SPE while calculating position corrections for the flight idle stalls. While in a clean configuration, it combined a level deceleration to sweep through Mach numbers, a constant-Mach roller coaster to sweep through a variety of AOAs, a 360-degree minimum level turn to estimate winds aloft, and in most cases ended in a clean stall to determine aircraft stall speed. The level deceleration started near a

[1] Numerals following an R represent recommendation numbers.

maximum level speed of about 220 KIAS with the power at flight idle to decelerate at a constant altitude down to an initial target Mach. At this target Mach, the power was increased to hold that Mach and pressure altitude. A roller coaster was flown at the target Mach to collect AOA data from 0.5 g to 1.8 g, allowing for more AOA variation than that caused solely by weight and speed changes. Following the roller coaster, a constant altitude 360-degree minimum turn was accomplished at the target Mach to determine an average wind vector. Following the turn, the level deceleration was continued at flight idle from the target Mach down to 1.5 V_{stall}. After reaching 1.5 V_{stall} and trimming to 1.5 V_{stall}, a non-level flight-idle deceleration was continued to stall as described below. Data from the "Angry Silv" maneuvers were used to determine SPE as a function of AOA and Mach number. Figure 7 provides a visual depiction of the "Angry Silv" FTT. The test team accomplished 42 "Angry Silv" maneuvers in the DAS aircraft at the three weight bands, three altitudes, and four target Mach numbers shown in Table 1, all in clean configuration. The details of the statistical analysis done on the "Angry Silv" data to examine the SPE predictor variables are shown in Appendix C.

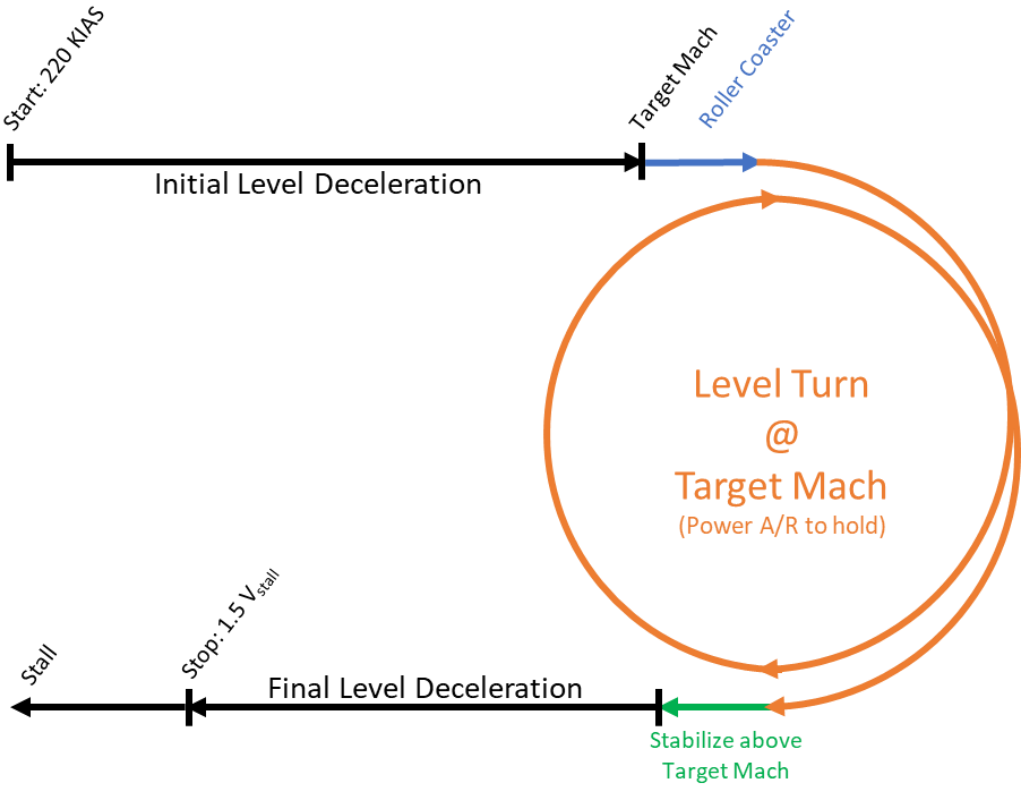

Figure 7. Graphical depiction of the "Angry Silv" FTT

Table 1. DAS Aircraft Test Condition Matrix

Gross Weight Band (pounds)	Pressure Altitudes (feet)	Target Mach Numbers
10,500-11,100 11,100-11,800 11,800-12,500	8500 PA ± 500 ft 14,000 PA ± 500 ft 19,500 PA ± 500 ft	0.25 0.30 0.35 0.40

Flight Idle Stalls

On the DAS aircraft, stall tests were conducted at flight idle power and 2000 propeller revolutions per minute (RPM) with wings level at the weights and altitudes listed in Table 1. The test team accomplished 33 clean stalls, 36 approach configuration stalls, and 34 landing configuration stalls. A clean configuration stall was completed at the end of most "Angry Silv" maneuvers described above. Independent stall test points in various configurations were also flown after the clean stall in the same airspace as the "Angry Silv" FTT. If not completed after an "Angry Silv" FTT, a minimum 360° turn was flown preceding stalls in the same airspace to facilitate SPE calculation.

In the non-DAS aircraft, stalls were performed at approximately 8,500 ft PA as listed in Appendix E, Table E1. Five stalls in clean configuration and six stalls in each of approach and landing configuration were flown. Position corrections derived from the flight manual performance appendix (reference 7) were applied to the non-DAS data to determine calibrated stall speeds. The DAS production Pitot-static system instrument-corrected flight test stall speeds were compared to the non-DAS instrument-corrected flight test stall speeds to confirm the applicability of the DAS aircraft results to a production model, per Appendix C.

The stall and stall recovery procedures followed the steps outlined in the program test plan (reference 1) and are listed in Appendix B. The stall speed was the speed at a definitive pitch break or at the minimum speed after the yoke reached the full aft position for up to two seconds without a pitch break. The aircraft center of gravity (CG) for all stalls was between 0-20 percent of the allowable CG range from the front of the aircraft. The forward CG maximized the control authority required during the stall. This increased the likelihood of a stall defined by aft yoke, which would occur at a higher speed than an aerodynamic stall, in order to collect the most conservative data. All stall data collected was a result of a definitive pitch break during these test flights, indicating that CG was not a factor.

Position Correction Calculations

To calculate calibrated airspeeds, position corrections were determined using a combination of air data methods. The details of this analysis and the air data methods briefly described below are shown in Appendix C.

Tower Flyby

The tower flyby FTT provided low altitude test data and was the traditional method to determine single-point SPEs. It was performed per the test plan by flying down the tower flyby line at approximately 200 feet AGL. Abeam the tower, data were recorded with indicated pressure altitude being the most important. At the same time, a test team member in the flyby tower recorded aircraft height and other handheld data using a theodolite. Nine tower flybys were accomplished on the DAS aircraft targeting 140, 180, and 240

knots and 200 to 250 feet AGL, at gross weights from 10,800 to 12,000 pounds. Handheld data from the tower flybys is shown in Table D5.

JMOSS Self-Contained Algorithm

The JMOSS algorithm used data from the "Angry Silv" maneuvers to determine SPE and the airspeed position corrections at stall in a self-contained mode. It also estimated the temperature recovery factor K_t using total temperature measurements from the aircraft and atmospheric temperature models. JMOSS can accept weather balloon-measured temperature to calculate K_t, but this was less accurate than the self-contained output when compared to the tower flyby data. Self-contained JMOSS was the primary source of SPE for this project. A depiction of the inputs and outputs required by the JMOSS algorithm is shown in Figure C1.

Survey Method

The survey method was applied to data from the tower flyby and "Angry Silv" FTTs as a check of the SPE calculation, using the weather balloon data as a known atmospheric pressure measurement and the static pressure recorded by the DAS. The SPE was calculated directly from these two measurements.

DETERMINATION OF C-12C FLIGHT IDLE STALL SPEEDS

The first general test objective was to determine the stall speeds of C-12C EPIC aircraft at flight idle thrust conditions.

Determine Stall Speeds

The specific test objective was to determine the flight idle stall speeds in cruise (Flaps Up, Gear Up), approach (Flaps 40%, Gear Down), and landing (Flaps 100%, Gear Down) configurations.

Test Results

In flight, the test conductor marked the DAS file at the first indication of stall. During data analysis, the load factor and airspeed were plotted for 1 second before and after this event marker. The data point immediately prior to the g-break was used for the following analysis. These data were shown Tables D1-D3 in Appendix D, with one line for each of the 103 DAS aircraft stalls. Calibrated stall speeds were determined by correcting instrument-corrected stall airspeeds for static position error (SPE) using the SPE generated by the JMOSS self-contained algorithm on the flight test data. All stalls were flown with wings level, and stall speeds for bank angles other than zero were extrapolated. The details of the data analysis are shown in Appendix C.

Indicated stall speeds at gross weights from 10,500 pounds to 12,000 pounds were collected in each configuration. The total and static pressures, instrument-corrected DAS airspeed, instrument-corrected ADC 1 airspeed, and calibrated airspeed for each cruise-configured stall are listed in Appendix D, Table D1. The data for approach-configured stalls are listed in Appendix D, Table D2, and the data for landing-configured stalls are listed in Appendix D, Table D3. The DAS and production (ADC 1) instrument-corrected airspeed (V_{ic}) were determined by the following equation:

$$V_{ic} = \sqrt{\left(\frac{1}{\rho_{SL}}\right) 7P_{SL}\left(\left(\frac{P_t - P_s}{P_{SL}} + 1\right)^{\frac{2}{7}} - 1\right)}$$

Where:

$P_{SL} = 2116.2\ \text{lb/ft}^2$ is the atmospheric pressure at sea level
P_s is the static pressure measured by the production system
P_t is the total pressure measured by the production system or boom
$\rho_{SL} = 0.0023769\ \text{slugs/ft}^3$ is the standard sea level density

The total boom pressure and production static pressure were used to determine the DAS V_{ic}. The production total and static pressures were used to determine the production (ADC 1) V_{ic}. The calibrated airspeed (V_c) was determined for each stall using the equation:

$$V_c = V_{ic} + \Delta V_{pc}$$

Where V_{ic} is the DAS instrument-corrected stall airspeed computed previously, and ΔV_{pc} is the velocity position correction derived from the JMOSS algorithm. The calibrated airspeeds (V_c) were calculated using these methods for each stall. Since the f-factor, used to convert equivalent to calibrated airspeeds, is approximately 1 across the C-12 operating envelope, $V_c = V_e$ (where V_e is the equivalent airspeed). The calibrated stall airspeeds above can be considered equivalent airspeeds.

This relationship allows the lift coefficient, $C_{L_{max}}$ to be determined for each stall by the following equation.

$$C_{L_{max}} = \frac{nW}{\frac{1}{2}\rho V_t^2 S} = \frac{nW}{\frac{1}{2}\rho_{SL} V_{e_{stall}}^2 S}$$

Where:

n is the load factor
W is the aircraft weight
S is the planform area of the aircraft, 303 ft^2 per the flight manual (reference 7)

The load factor, n, was found from the bank angle, ϕ, assuming that the aircraft is flying level.

$$n = \frac{1}{\cos\phi}$$

The $C_{L_{max}}$ was calculated for each stall. All stalls were characterized by a g-break, therefore the $C_{L_{max}}$ for each configuration of stall was averaged to determine a $C_{L_{max}}$. All of the clean stall $C_{L_{max}}$ values were averaged to determine a single, clean configuration value. This was also done to determine an approach configuration $C_{L_{max}}$ value and a landing configuration $C_{L_{max}}$ value. Table 2 shows the $C_{L_{max}}$ values for each configuration.

Table 2. Average $C_{L_{max}}$ for Each Aircraft Configuration

	Clean Configuration (Flaps 0%, Gear – Up)	**Approach Configuration (Flaps 40%, Gear – Down)**	**Landing Configuration (Flaps 100%, Gear – Down)**
Average Maximum Lift Coefficient, $C_{L_{max}}$	1.31	1.65	2.10

These three $C_{L_{max}}$ values were used to determine stall speeds ($V_{c_{stall}}$) at the weights and bank angles required for Figures 6-1 and 6-2 in the flight manual by using the following equation:

$$V_{c_{stall}} = \sqrt{\frac{nW}{\frac{1}{2}\rho_{SL} C_{L_{max}} S}}$$

Since the flight manual must match C-12 indicated airspeeds, production total pressure and static pressure at stall were taken to compute $V_{ic_{stall}}$ using the formula in Appendix C. $V_{ic_{stall}}$ was plotted against $V_{c_{stall}}$ for each configuration in figures D1, D2, and D3 of Appendix D. A simple linear regression fit was used to model the relationship between these two speeds, with one model fit for each aircraft configuration as shown in each of the figures in Appendix D. The production-representative instrument-corrected stall speeds were then determined using the linear regression model between $V_{ic_{stall}}$ and $V_{c_{stall}}$.

Based on the flight test stall values and the JMOSS position corrections, an updated table for Figure 6-1 in the C-12C flight manual was generated. Figure 8 shows the current table from the 1C-12A-1 Change 4, 15 July 2020. The proposed updated table based on flight test data is shown in Figure 9.

TAKEOFF/CRUISE

POWER: IDLE
FLAPS: UP LANDING
GEAR: UP OR DOWN

GROSS WEIGHT	STALL SPEEDS – KNOTS IAS ANGLE OF BANK				
	0°	15°	30°	45°	60°
10,500	81	83	87	97	113
11,000	84	86	90	100	119
11,500	86	88	92	102	121
12,000	89	91	96	106	125
12,500	91	93	98	108	127

APPROACH

POWER: IDLE
FLAPS: APPROACH LANDING
GEAR: DOWN

GROSS WEIGHT	STALL SPEEDS – KNOTS IAS ANGLE OF BANK				
	0°	15°	30°	45°	60°
10,500	72	74	77	85	101
11,000	74	76	80	88	104
11,500	76	78	82	90	106
12,000	78	80	84	94	110
12,500	81	83	87	97	113

LANDING

POWER: IDLE
FLAPS: FULL DOWN
LANDING GEAR: DOWN

GROSS WEIGHT	STALL SPEEDS – KNOTS IAS ANGLE OF BANK				
	0°	15°	30°	45°	60°
10,500	65	66	70	77	92
11,000	67	68	72	79	94
11,500	68	69	74	81	97
12,000	70	71	75	83	99
12,500	71	73	76	84	100

Figure 8. 1C-12A-1 Figure 6-1

TAKEOFF / CRUISE

POWER: IDLE
FLAPS: UP LANDING
GEAR: UP OR DOWN

GROSS WEIGHT	STALL SPEEDS – KNOTS IAS ANGLE OF BANK				
	0˚	15˚	30˚	45˚	60˚
10,500	92	94	99	110	131
11,000	94	96	101	112	133
11,500	95	97	102	113	135
12,000	97	98	104	115	137
12,500	98	100	106	117	139

APPROACH

POWER: IDLE
FLAPS: APPROACH LANDING
GEAR: DOWN

GROSS WEIGHT	STALL SPEEDS – KNOTS IAS ANGLE OF BANK				
	0˚	15˚	30˚	45˚	60˚
10,500	81	82	87	96	114
11,000	82	83	88	98	116
11,500	83	85	89	99	118
12,000	85	86	91	101	120
12,500	86	87	92	102	121

LANDING

POWER: IDLE
FLAPS: FULL DOWN
GEAR: DOWN

GROSS WEIGHT	STALL SPEEDS – KNOTS IAS ANGLE OF BANK				
	0˚	15˚	30˚	45˚	60˚
10,500	71	72	76	84	100
11,000	72	73	77	85	101
11,500	73	74	78	86	103
12,000	73	75	79	87	104
12,500	74	75	80	88	105

Figure 9. Proposed Figure 6-1 Update

As expected based off of the previously noted stall discrepancies, the instrument-corrected airspeeds at stall were higher than the values published in the flight manual. A proposed updated graph for Figure 6-2 in the C-12C flight manual was also generated. The current graph from the 1C-12A-1 Change 3, 31 July 2017 is shown in Figure 10 below, with the proposed update in Figure 11. An expanded version of Figure 11 is shown in Appendix D.

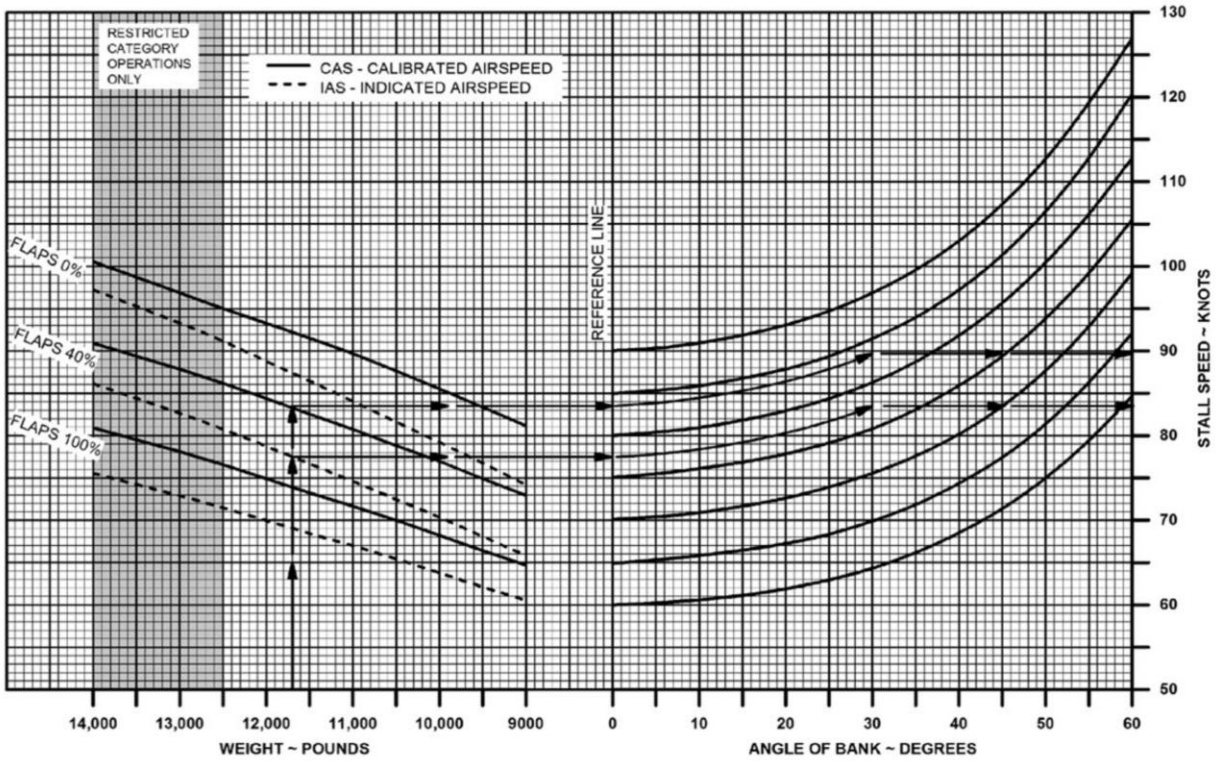

Figure 10. 1C-12A-1 Figure 6-2

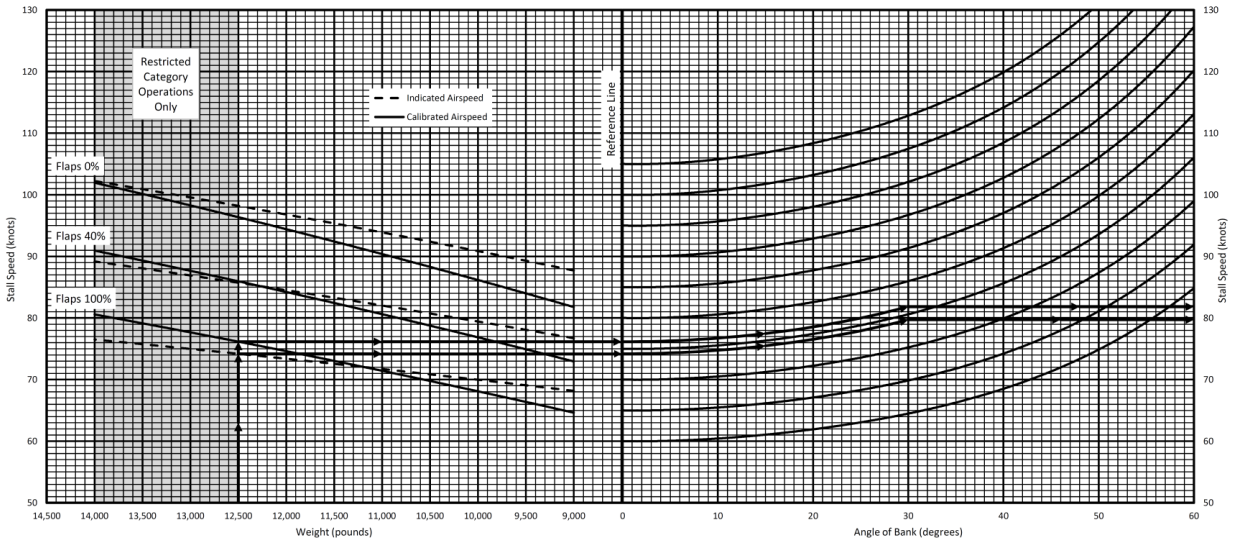

Figure 11. Proposed Figure 6-2 Update

As shown above, the stall speeds determined during this program were found to be significantly higher than the published figures in the current C-12C flight manual. Consequently, the flight manual should be updated to ensure safety of flight. **Update C-12C flight manual stall speed figures to reflect the higher stall speeds determined during this program. (R1)** Additionally, these stall speeds may impact other performance measures such as rotation speed, takeoff safety speed, or approach speed. Per ASTM F3179 (reference 5), the current FAA standard regarding performance speeds, rotation speed shall not be less than 1.1 V_{stall}. The flight manual (reference 7) gave a rotation speed of 94 KIAS for all non-restricted weight

flaps up takeoffs, which was less than 1.1 V_{stall}. Based on the recommended stall speed updates, flaps up rotation speeds should increase from 94 KIAS to a range from 98 KIAS to 108 KIAS based on takeoff weight. **Recommend the SPO investigate the implications of increased flight idle stall speeds on TOLD calculations. (R2)**

Compare Stall Speeds

The specific test objective was to compare a sample of C-12C flight idle stall speeds between non-DAS and DAS EPIC-configured aircraft.

Test Results

The instrument-corrected airspeeds from the production system of the DAS aircraft, calculated above, were compared to the instrument-corrected airspeeds of the non-DAS aircraft. On the non-DAS aircraft, instrument corrected airspeeds were determined by recording the indicated airspeed (V_i) from ADC 1 and applying the instrument correction (ΔVic) found in Table A5 to determine the instrument-corrected airspeed (V_{ic}) using the following equation.

$$V_{ic} = V_i + \Delta V_{ic}$$

This was performed for each of the indicated airspeeds collected for a total of 17 stalls in the non-DAS aircraft. Stalls were performed between 8,000 and 9,000 feet PA and 10,850 and 11,800 pounds gross weight. Table D4 lists the specific conditions, as well as the indicated and instrument-corrected airspeeds for each stall.

Figure 12 shows the DAS stall speeds, the ADC stall speeds from the DAS aircraft, the ADC stall speeds from the non-DAS aircraft, and the stall speeds from the flight manual for an EPIC-modified aircraft, with instrument-corrected indicated speeds in the top row of plots and calibrated speeds in the bottom row. The instrument-corrected stall speeds derived from the production ADC appear similar between the DAS and non-DAS aircraft with the exception of the approach configuration, where the non-DAS stall speeds are slightly slower. However, all stall speeds were higher than the EPIC stall speeds. As the DAS system stall speeds differed by approximately three knots, the ADC stall speeds were judged to be more representative of the fleet. With the exception of the approach configuration, calibrated stall speeds were almost identical between the two aircraft. This indicated that the stall data were likely fleet representative.

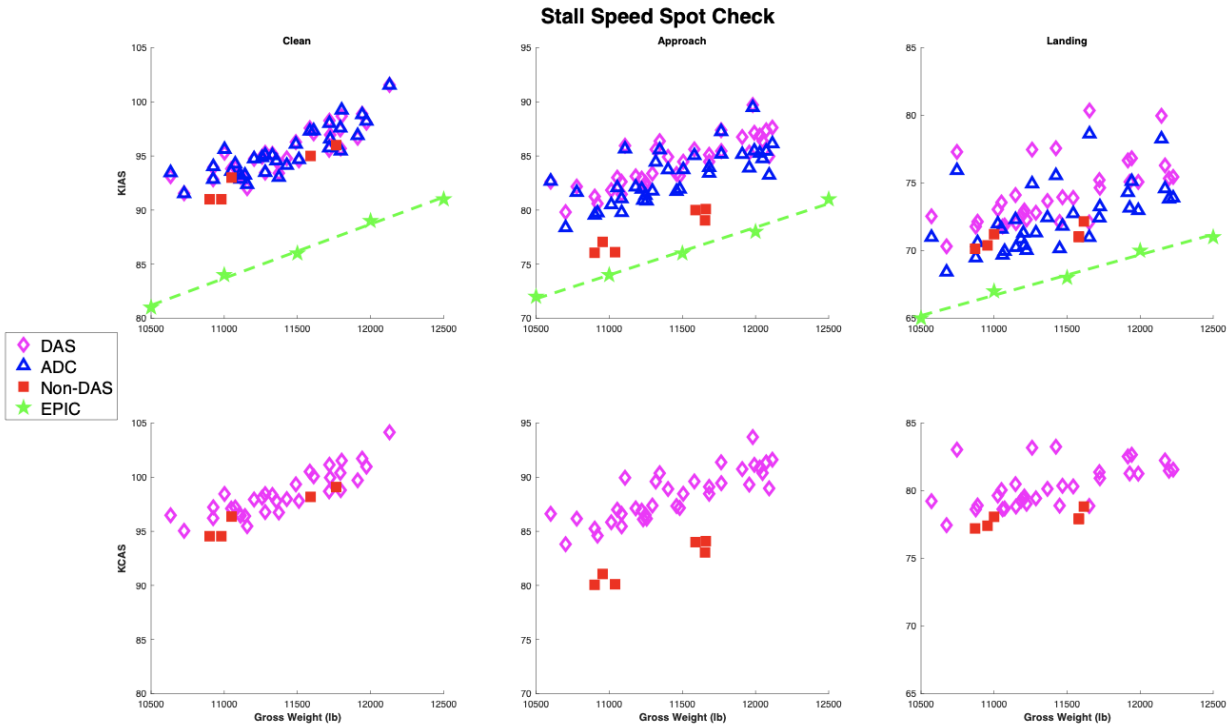

Figure 12. Instrument-Corrected Production, Instrument-Corrected DAS, Calibrated, and Flight Manual Stall Speeds for DAS and Non-DAS Aircraft

Additionally, normally distributed statistical hypothesis tests were performed to confirm that the observed instrument-corrected stall speeds samples from the non-DAS aircraft were not statistically different from those observed in the ADC dataset from the DAS aircraft. The clean and landing configurations showed no statistically significant difference in the means of stall speeds of DAS and non-DAS aircraft, as shown in Figure 13. The approach-configured stall speeds had four of the six stall speeds within the 95% confidence interval. This indicates that at the 95% confidence level, the non-DAS aircraft stall speeds matched the DAS stall speeds, validating the assumption that the DAS system and the flight test nose boom did not significantly alter the stall speeds, and more importantly, that the collected DAS stall speeds can be considered fleet-representative.

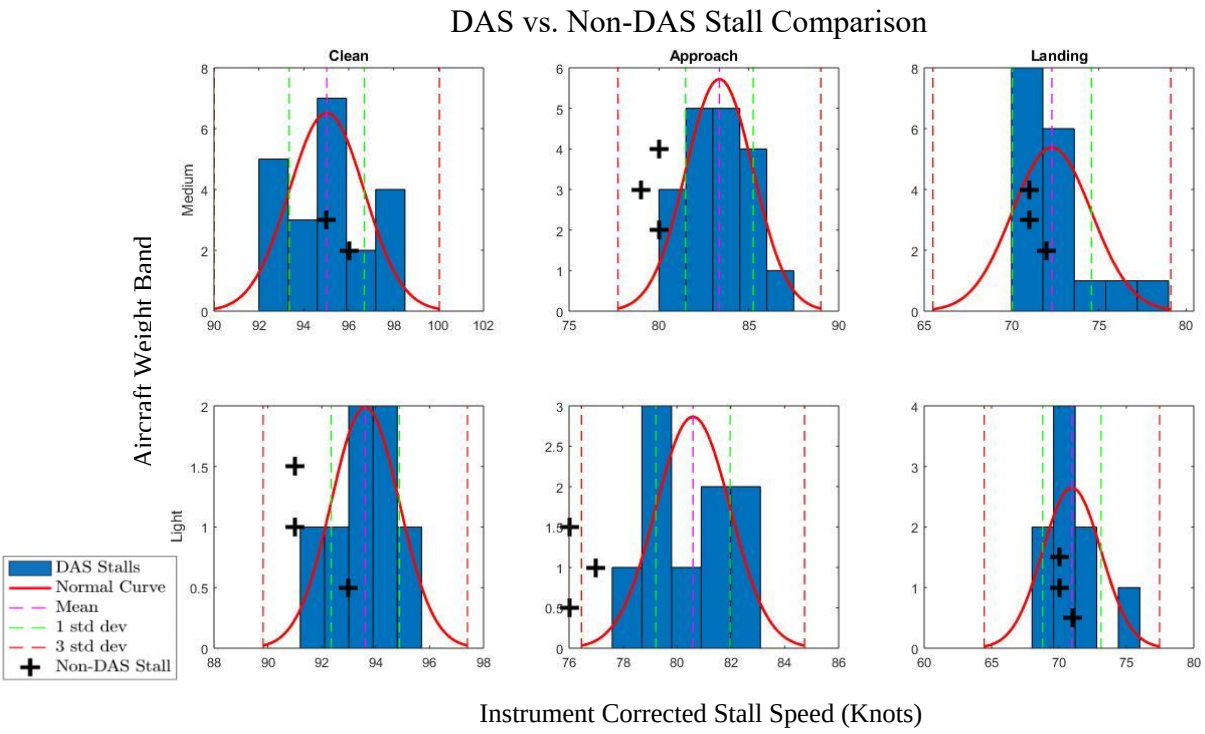

Figure 13. Hypothesis Testing the Non-DAS Data.

DETERMINATION OF SPE AS A FUNCTION OF AOA AND MACH

The second general test objective was to determine the static position error as a function of angle of attack and Mach number.

AOA, Mach, and Interaction Significance

The specific test objectives were to determine the statistical significance of angle of attack, Mach number, and the interaction of angle of attack and Mach number on static position error.

Test Results

In initial modeling of all factors and interactions, the p-values of angle of attack (α), Mach, and α*Mach were determined to be $p < 0.001$. This indicated a statistically significant relationship; there is a near zero probability that the observed AOAs, Mach numbers, and SPEs happened simultaneously by random chance. To further assess the effect on SPE, the decision was made to assess the model by measuring how much model variance was explained by each parameter. The team explored the main effects of combinations of the variables iteratively and reported an analysis of covariance (ANCOVA) as well as a generalized linear model (GLM). Table 3 shows the initial GLM.

Table 3. Initial GLM of $\Delta P_p/P_s$ by AOA, Mach

Generalized Linear Model Coefficients of $\Delta P_p/P_s$ by Alpha, Mach							
Covariate	β	p-value	Std Error	t	CI Lower	CI Upper	Part. η^2
Intercept	-0.016	<0.001	0.000	-108.285	-0.016	-0.015	0.033
Mach	0.102	<0.001	0.001	95.832	0.100	0.104	0.026
α	0.006	<0.001	0.000	43.916	0.006	0.007	0.006
$Mach^2$	-0.207	<0.001	0.002	-99.458	-0.211	-0.203	0.028
α^2	4.691	<0.001	0.080	58.510	4.534	4.848	0.010

Type III sum of squares (SS) were used to adjust for all effects, meaning that each variable was assessed as if it were the last after accounting for the effects of the other variables. Overall model effectiveness was measured using the coefficient of determination (r^2). Parameter effect was measured using partial Eta-Squared (η^2), the ratio of variance explained in the dependent variable by a given predictor. In the initial GLM, AOA only had a partial η^2 of 0.006, indicating that as a standalone variable, it did not account for any significant amount of model variance. Consequently, the standalone variable of AOA was omitted from the final GLM shown in Table 4. Intercepts were also omitted from this final model, assuming that at zero Mach number and angle of attack, SPE would also be zero.

Table 4. Final GLM of $\Delta P_p/P_s$ by AOA, Mach

Generalized Linear Model Coefficients of $\Delta P_p/P_s$ by Alpha, Mach							
Covariate	β	p-value	Std Error	t	CI Lower	CI Upper	Part. η^2
Mach	-0.006	<0.001	1.02E-05	-613.956	-0.006	-0.006	0.632
α*Mach	0.049	<0.001	0.000	166.992	0.049	0.05	0.113
α^2 (sign retained)	-0.044	<0.001	0.000	-105.494	-0.044	-0.043	0.048

Table 4 also shows the significance, effect, and variance data of the variables and their interactions on the GLM. The relationship between SPE and Mach was the strongest; the Mach parameter was predicted to explain 63% of the model variance with a partial η^2 of 0.632. The relationships of SPE to interactions of Mach and AOA were observed in $\alpha * Mach$ and α^2 (sign retained). "Sign retained" meant the original sign of the variable is kept in the expression after applying operators. The variable $\alpha * Mach$ accounted for 11% of model variance (partial $\eta^2 = 0.113$). The variable α^2 also had a significance of $p < 0.001$, but only covered 5% of the model variance (partial $\eta^2 = 0.048$). All interactions of angle of attack and Mach were statistically significant factors of SPE, but further parameters neither exhibited strong partial η^2 nor increased the coefficient of determination (r^2) described in the ANCOVA analysis in Table 5. They were therefore omitted from the model.

Table 5. ANCOVA of $\Delta P_p/P_s$ by Alpha, Mach

Analysis of Covariance (ANCOVA) of $\Delta P_p/P_s$ by Alpha, Mach				
Source of Variance	Adjusted SS (Type III)	Degrees of Freedom	Mean Square	F
Model	0.775	3	0.258	132368.656*
Mach	0.736	1	0.736	376942.067*
$\alpha \cdot Mach$	0.054	1	0.054	27886.282*
α^2 (sign retained)	0.022	1	0.022	11128.931*
Error	0.428	219270	1.95E-06	
$r^2 = 0.644$			* $p < 0.05$	

For a model with the three variables shown above and 219,270 error degrees of freedom as calculated by the number of discrete DAS/TSPI data points less the number of variables, the F-statistic was 132368.66. The F-statistic could be thought of as an inverse p-value, where a large value implies that the model mean was representative of the data set. The large F statistics seen showed that the SPE within the model also had a very low probability of occurring by chance, and that the p-value of the GLM of SPE was also significant to a $p < 0.001$ level. Additionally, the r^2 of 0.644 indicated a correlation of variables accounting for 64% of model variance. However, this was insufficient to predict SPE from only Mach and AOA in all flight environments, implying that other variables must also have been contributors. Further details of the GLM analysis are provided in Appendix C.

Overall, the test team assessed that Mach was a good predictor of SPE but that AOA alone did not add any fidelity to the model. JMOSS provided an efficient and self-contained platform for this analysis.

Additional Findings

The customer was interested in the difference of performance between the raw data of the self-contained JMOSS mode and the JMOSS mode that incorporates weather balloon temperatures. Additionally, tower flyby SPE was computed using the GLM and traditional tower flyby methods, and the survey method SPE was computed using traditional survey methods. These methods are all described in Appendix C. The mean square error (MSE) of SPE, as defined in Appendix C was used to compare the self-contained JMOSS (with derived temperature recovery factor), the JMOSS with balloon temperatures, and survey data to show the differences of accuracy. Table 6 shows the results of the comparison. The variable $\mu\Delta\Delta V_{pc}$ was the mean difference in ΔV_{pc} computed from the static position error root MSE. As expected, JMOSS SPE using balloon temperature was closer to the survey SPE that relied entirely upon balloon data than self-contained JMOSS.

The mean difference of the tower flyby to the model predicted values appeared to be as an anomaly, leading the test team to conduct further investigation into the cause. The barometer used to measure pressure altitude in the flyby tower was determined to be incorrectly calibrated. Spot checks conducted by the test team showed discrepancies of 50 feet, and the team technical expert cited discrepancies of up to 66 feet (reference 14). In all cases the tower flyby barometer read altitudes higher than the actual pressure altitude. To explore the effects of this error on the tower flyby data, the test team reanalyzed the tower flyby using heights 66 feet lower than what were collected during the tower flybys to include mean differences in ΔV_{pc} for TFB (corrected).

Table 6. MSE Across SPE Collection Types & ΔV_{pc} Error

Mean Square Error Across SPE Collection Types				
Variable	Self-Contained JMOSS vs. Survey	Balloon JMOSS vs. Survey	GLM vs. TFB	GLM vs. TFB (corrected)
$\frac{\Delta P_p}{P_s}$ MSE	2.486E-06	1.536E-06	1.455E-05	3.059E-06
$\mu\Delta\Delta V_{pc}$ (at TFB conditions)	2.35 kts	1.38 kts	5.65 kts	2.61 kts

Figure 14 clearly shows that this data correction brought the tower flyby data within the prediction intervals of the GLM, and that it matched with the plurality of JMOSS collected SPEs. The Digital Data Appendix contains a 3D version of this figure.

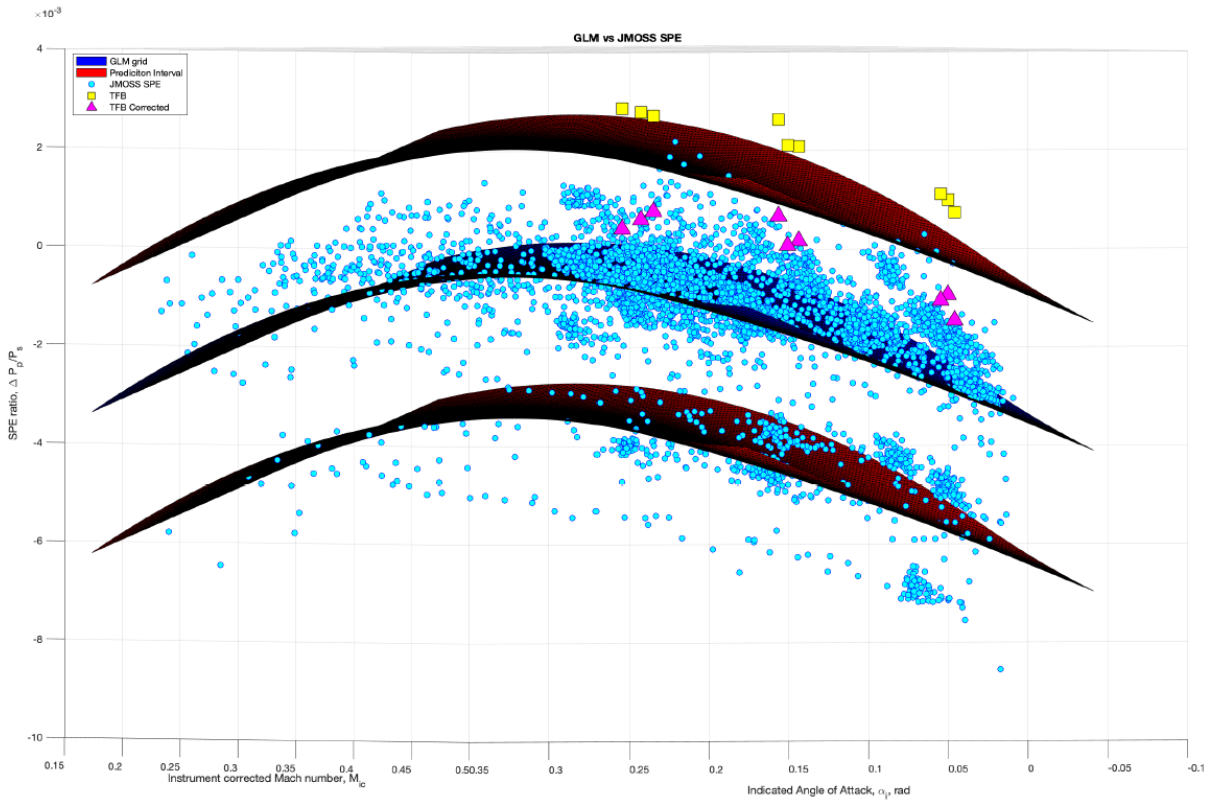

Figure 14. GLM Prediction Intervals and TFB Corrections

The test team conducted a preliminary investigation into other variables as predictors, using altitude, weight, torque, and exhaust gauge temperature, as standalone indicators, and observed $r^2 = 0.75$ with some immature modeling of additional effects. This indicated to the test team that further research into SPE modeling could explain more of the variance in SPE values observed.

TEST RESULTS SUMMARY

The Have EPIC DISCO test results showed that the wings level stall speeds of EPIC-modified C-12C aircraft were as much as seven knots higher than the stall speeds currently published in the aircraft flight manual. Stall testing in the fleet representative C-12C also revealed few statistically significant differences between the stall speeds of DAS and non-DAS aircraft, with all stall speeds higher than EPIC numbers. This means that the flight test boom did not significantly alter the stall speed and that the collected DAS stall speeds can be considered fleet-representative. Additionally, the Jurado-McGehee Online Self Survey method successfully determined the static position error of the C-12C and revealed the relationship of static position error to Mach and angle of attack. Although both variables exhibited a statistically significant relationship, AOA was not found to have a strong effect on the SPE variance and was not a good predictor of SPE in the C-12C. The test team recommends that the stall speeds in the C-12C flight manual should be updated to reflect the higher stall speeds discovered during this test program.

REFERENCES

1. *Position Corrections and Stall Characteristics of EPIC Modified C-12C,* USAFTPS-TP-20A-03, August 2020.

2. *Flying Qualities for Piloted Aircraft,* MIL-STD-1797B.

3. ASTM Compliance Standard F3180/F3180M, *Standard Specification for Low-Speed Flight Characteristics of Aircraft,* 1 June 2018.

4. Advisory Circular: Flight Test Guide for Certification of Part 23 Airplanes, AC 23-8C, U.S. Department of Transportation, Federal Aviation Administration, 16 November 2011.

5. ASTM Compliance Standard F3179/F3179M, *Standard Specification for Performance of Aircraft,* 1 May 2018.

6. Preliminary Test Results, PIRATE SNAIL PACER Test Program, emailed by Mr. Karl Major, 4 August 2020.

7. *Flight Manual USAF Series Aircraft C-12C/C-12D,* T.O. 1C-12A-1 Change 4, 15 July 2020.

8. Fli*ght Manual USAF Series Aircraft C-12C/C-12D,* T.O. 1C-12A-6CF-1, 31 May 2017.

9. MEMORANDUM FOR Edwards AFB C-12 Operators, 412 OG/CC, June 2017.

10. PIRATE SNAIL PACER Test Package, 201700300, March 2017.

11. Jurado, J. & McGehee, C. (2018). Complete Online Algorithm for Air Data System Calibration. Journal of Aircraft. 56. 1-12. 10.2514/1.C034964.

12. HAVE SPEED Test Report, USAF TPS-TIM-17A-02, December 2017.

13. Jurado. J. Air Data Academics, USAF TPS, presented to TMP group 31 May 2020.

14. See a copy of the email in the Digital Data Appendix sent from Mr. Chuck Webb, Technical Expert, to Lt Col Silv Jurado, TPS Education Director, 1 Dec 2020, concerning the calibration of the TPS tower flyby altimeter.

15. *Modification Flight Manual C-12C 76-0158,* Change 1, 1 October 2014.

16. R.E. Erb. *Pitot-statics and the Standard Atmosphere, 4th Edition,* USAF TPS, July 2020.

This page was intentionally left blank.

APPENDIX A – ADC GROUND CALIBRATION

DAS CONFIGURED GROUND CALIBRATION

Ground calibration took place on 1 September 2020 and consisted of connecting the Druck™ Air Data Test System (ADTS) 405 (Figure A1) to Air Data Computer (ADC) 1 (Figure A2) and the Data Acquisition System (DAS). The DAS was connected directly to the ADC 2 static port, but has its own total pressure port. The altimeter was set to 29.92 in. Hg. Various pressures were dialed into the Druck™ ADTS 405 to simulate changes to airspeed and altitude for the ADC. The resulting values displayed by the ADC were recorded by hand to determine the instrument corrected altitude and airspeed. The instrument corrections were calculated by subtracting the indicated airspeed and altitude from the truth airspeed and altitude. These values were recorded at the simulated altitude and airspeed conditions in Tables A1-A4. The DAS altitude was reported in inches of mercury and were converted to pressure altitudes using:

$$H_c = \frac{1 - \delta^{\left(\frac{1}{5.2559}\right)}}{6.87559 * 10^{-6}}$$

Where:

H_c is the pressure altitude

δ is the pressure ratio of Pressure / Pressure Sea Level

Figure A1. Druck™ ADTS 405

Figure A2. Druck™ ADTS 405 Connected to ADC 1

Table A1. ADC 1 Airspeed Instrument Corrections

	Airspeed (knots)												
Altitude (ft)	**60**	**70**	**80**	**90**	**100**	**110**	**120**	**140**	**160**	**180**	**200**	**220**	**240**
2500	-3.5	-3	-2.5	-2	-2	-1.5	-1	-1	-1.5	-1.5	-0.5	-0.5	-0.5
7500	-5	-4	-3.5	-3	-3	-2	-2	-2	-2	-2	-1	-1	-1
8000	-5	-4.5	-4	-3.5	-3	-2	-2	-2	-2	-2	-1	-0.5	-1
8500	-5	-4.5	-4	-3.5	-3	-2	-2	-2	-2	-2	-1	-1	-1
9000	-5	-4.5	-4	-3.5	-3	-2	-2	-2	-2	-2	-1	-1	-1
9500	-5	-5	-4	-4	-3	-2.5	-2	-2	-2	-2	-1	-1	-1
13000	-6	-5.5	-5	-4	-3	-3	-2.5	-2.5	-2.5	-2	-1.5	-1	-1
13500	-6	-5	-5	-4	-3.5	-3	-2.5	-2.5	-2.5	-2	-1.5	-1	-1
14000	-6	-5.5	-5	-4.5	-4	-3	-2.5	-2.5	-2.5	-2	-1.5	-1	-1
14500	-6.5	-6	-5	-4.5	-4	-3	-2.5	-3	-3	-2.5	-1.5	-1	-1
15000	-6.5	-6	-5	-4.5	-4	-3	-2.5	-2.5	-3	-2.5	-1.5	-1	-1
18500	-7.5	-6.5	-6	-5	-4	-3.5	-3	-3	-3	-2.5	-1.5	-1.5	-1.5
19000	-7	-6	-5.5	-5	-4	-3.5	-3	-3	-3	-3	-2	-1.5	-1.5
19500	-7	-6	-6	-5	-4.5	-3.5	-3	-3	-3	-3	-2	-1.5	-1.5
20000	-7	-6	-6	-5	-4.5	-3.5	-3	-3	-3	-3	-2	-1.5	-1.5
20500	-7	-6	-6	-5	-4.5	-3.5	-3	-3	-3	-3	-2	-1.5	-1.5

Table A2. ADC 1 Altitude Instrument Corrections

	Airspeed (knots)												
Altitude (ft)	**60**	**70**	**80**	**90**	**100**	**110**	**120**	**140**	**160**	**180**	**200**	**220**	**240**
2500	0	0	0	0	0	0	0	0	0	0	0	0	0
7500	0	0	0	0	0	0	0	0	0	0	0	0	10
8000	0	0	0	0	0	0	0	0	0	0	0	0	10
8500	0	0	0	0	0	0	0	0	0	0	0	0	0
9000	0	0	0	0	0	0	0	0	0	0	0	0	10
9500	0	0	0	0	0	0	0	0	0	0	0	0	10
13000	0	0	0	0	0	0	0	0	0	0	0	10	20
13500	0	0	0	0	0	0	0	0	0	0	0	10	20
14000	0	0	0	0	0	0	0	0	0	0	0	10	20
14500	0	0	0	0	0	0	0	0	0	0	0	10	20
15000	0	0	0	0	0	0	0	0	0	0	0	10	30
18500	0	0	0	0	0	0	0	0	0	0	10	20	40
19000	0	0	0	0	0	0	0	0	0	0	10	20	40
19500	0	0	0	0	0	0	0	0	0	0	10	30	50
20000	0	0	0	0	0	0	0	0	0	0	10	30	50
20500	0	0	0	0	0	0	0	0	0	0	20	30	50

It is unknown why altitude corrections changed at high speeds on the DAS aircraft, but these values were not used.

Table A3. DAS Airspeed Instrument Corrections

	Airspeed (knots)												
Altitude (ft)	**60**	**70**	**80**	**90**	**100**	**110**	**120**	**140**	**160**	**180**	**200**	**220**	**240**
2500	-1	-1	-0.5	-0.5	-0.5	0	0	0	0	0	0	0	0
7500	-1	-0.5	0	0	0	0	0	0	0	0	0	0	0
8000	-1	-0.5	0	0	0	0	0	0	0	0	0	0	0
8500	-0.5	-0.5	0	0	0	0	0	0	0	0	0	0	0
9000	-0.5	-0.5	0	0	0	0	0	0	0	0	0	0	0
9500	-0.5	-0.5	0	0	0	0	0	0	0	0	0	0	0
13000	-0.5	-0.5	0	0	0	0	0	0	0	0	0	0	0
13500	-0.5	-0.5	0	0	0	0	0	0	0	0	0	0	0
14000	-0.5	-0.5	0	0	0	0	0	0	0	0	0	0	0
14500	-0.5	-0.5	0	0	0	0	0	0	0	0	0	0	0
15000	-0.5	-0.5	0	0	0	0	0	0	0	0	0	0	0
18500	-0.5	-0.5	0	0	0	0	0	0	0	0	0	0	0
19000	-0.5	-0.5	0	0	0	0	0	0	0	0	0	0	0
19500	-0.5	-0.5	0	0	0	0	0	0	0	0	0	0	0
20000	-0.5	-0.5	0	0	0	0	0	0	0	0	0	0	0
20500	-0.5	-0.5	-0.5	0	0	0	0	0	0	0	0	0	0

Table A4. DAS Altitude Instrument Correction

Altitude (ft)	ΔH_{ic} (ft)
2500	-4
7500	-3
8000	-5
8500	-3
9000	3
9500	2
13000	-1
13500	-1
14000	5
14500	3
15000	7
18500	7
19000	8
19500	0
20000	1
20500	11

Tables A1-A4 were not used in the calculation of instrument-corrected stall speed, as these speeds were directly derived from pressure values. However, this information is presented here for completeness.

NON-DAS CONFIGURED GROUND CALIBRATION

Ground calibration took place on 24 September 2020 and was the same setup and procedure as during the DAS configured ground calibration. Ground calibration took 20 minutes. The instrument corrections were recorded at the simulated altitude and airspeed conditions in Tables A5-A6. Ground calibration requirements were reduced for altitudes between 8,000 – 9,000 ft. pressure altitude because stalls were only accomplished between those altitudes in the non-DAS configured aircraft.

Table A5. Non-DAS ADC 1 Airspeed Instrument Correction

	Airspeed (knots)					
Altitude (ft)	**60**	**70**	**80**	**90**	**100**	**110**
8000	0	0	0.5	0	0	0.5
8500	0	0	0	0	0	0.5
9000	0	0.5	0	0	0	0.5

Table A6. Non-DAS ADC 1 Altitude Instrument Correction

Altitude (ft)	ΔH_{ic} (ft)
8000	-20
8500	-20
9000	-20

This page was intentionally left blank.

APPENDIX B – DETAILED TEST ITEM DESCRIPTION

The C-12C was a twin engine power turbine aircraft operating between 1600 to 2000 RPM. It was primarily used to transport people or cargo. Figure B1 shows the size and dimensions of the aircraft. The information below could be found in the flight manual (reference 7) and modified flight manual (reference 15).

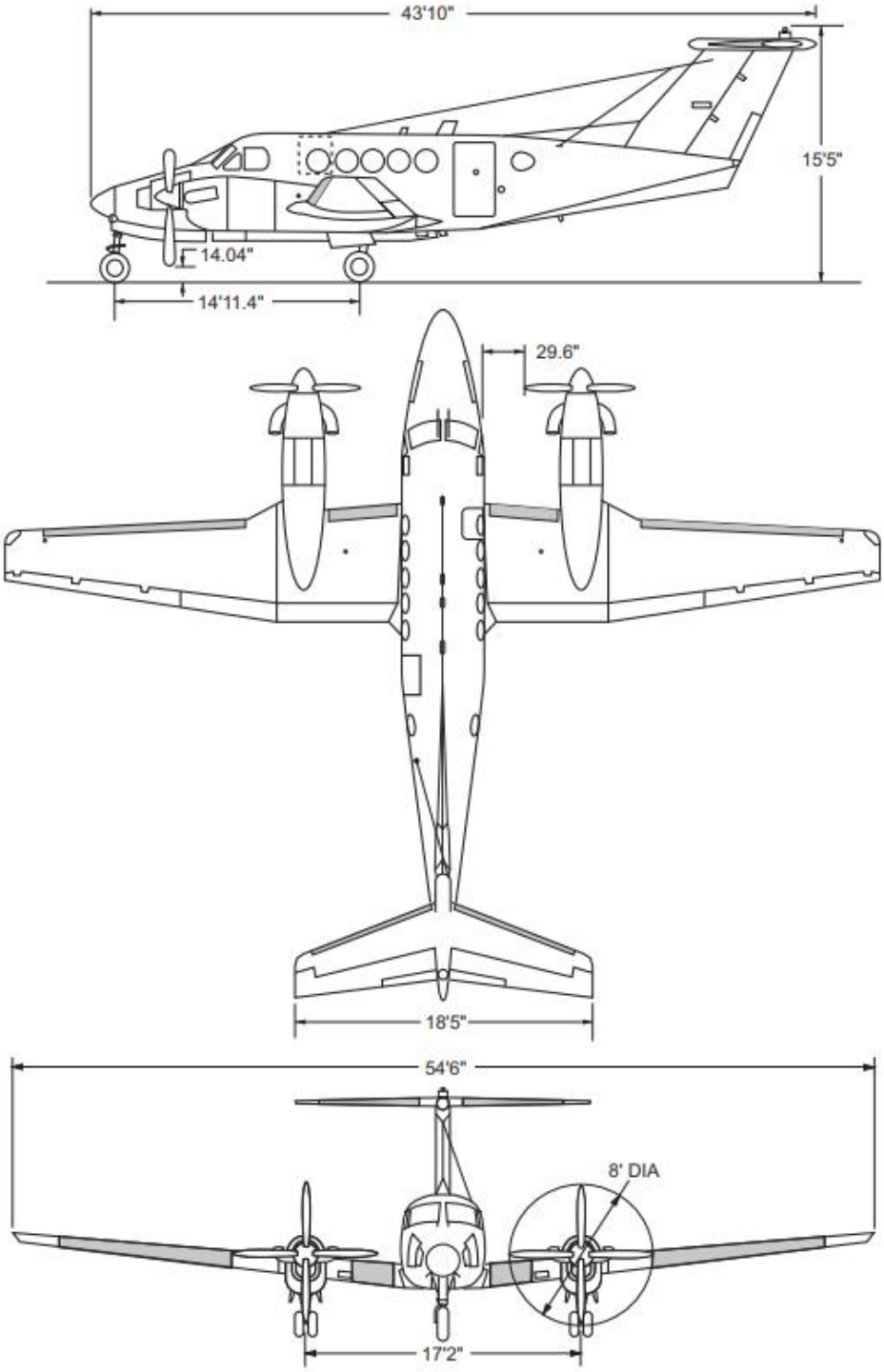

Figure B1. C-12C Three view drawing

PROPELLERS

The C-12C used two Hartzell four-bladed swept blade turbofan propellers. The propellers were manufactured with aluminum hubs and blades mounted to the output shaft of the reduction gearbox and were full-feathering, constant speed, counter weighted, reversing, variable pitch, and were controlled by engine oil through a primary governor.

PRODUCTION PITOT STATIC SYSTEM

The Pitot and static system provided a source of impact air and static air for the Air Data Computers (ADC1 and ADC2). A Pitot mast was located on each side of the lower portion of the nose. Tubing from each mast extended into the nose avionics bay to the associated computers. Information from the left Pitot mast was provided to ADC1 as well as the ESIS and similar information from the right Pitot mast was provided to ADC2 and the Flight Data Recorder (FDR). There were four normal static system ports with two each located on the left and right side of the rear fuselage aft of the rear pressure bulkhead. The four normal static ports provided two separate sources of static air; one for the pilot's system and one for the copilot's. Each of the normal static air system lines opened to the atmosphere through two static air ports; one on each side of the fuselage. The pilot's side received static information from the upper left and lower right ports and provided this information to ADC1, the ESIS, and the Autopilot Computer. The copilot's side received static information from the upper right and lower left ports and provided this information to ADC2, the FDR, and the Autopilot Computer. These ports were not heated. There were three drain petcocks located on the right lower sidewall used for draining the static air lines. These drain valves were opened by maintenance to release any trapped moisture during a routine scheduled inspection.

STALL WARNING SYSTEM

The stall warning system consisted of a transducer, a lift computer, a warning horn, and a test switch. Angle of attack was sensed by aerodynamic pressure on the lift transducer vane located on the left wing leading edge. When a stall was imminent, the output of the transducer sent a signal to the stall warning computer which in turn activated the stall warning horn and sent a digital discreet signal to the autopilot to disconnect. The system had preflight test capability through the use of a switch placarded STALL WARN TEST - OFF - LANDING GEAR WARN TEST on the right subpanel. Holding this switch in the STALL WARN TEST position actuated the warning horn by moving the transducer vane. The lift transducer was equipped with anti-icing capability on both the mounting plate and the vane.

PRIMARY FLIGHT DISPLAY

The Primary Flight Display (PFD), Figure B2, displayed pitch, roll, heading, airspeed, airspeed targets, vertical speed, altitude, altitude pre-select target, vertical speed, radio altitude, decision altitude/radio altitude minimums, flight guidance steering commands, flight guidance modes, auto-pilot/yaw damper modes, lateral/vertical deviation steering cues and warning/caution annunciators.

Figure B2. PFD

DATA ACQUISITION SYSTEM

The DAS consisted of the Instrumentation Master Power System, the DAS rack (Figure B3), Attitude Heading and Reference System (AHRS) tray, Flight Test Engineer (FTE) console with keyboard and mouse, special instrumentation sensors, C-Band Telemetry Transmitter, taps into several production Electronic Flight Instrument System (EFIS) ARINC-429 avionics busses, flight test nose boom and a C-Band beacon transponder. Data recording was performed by a Teletronics Technology Corporation (TTC) solid state recorder (SSR) onto a removable flash drive.


Figure B3. DAS Rack

STALL AND RECOVERY PROCEDURES

The stall procedures used during this test were as follows:

1) Verify altimeter set to 29.92 in. Hg.
2) Trim aircraft at 1.5 times the predicted stall speed for a clean stall, or 1.3 times the predicted stall speed for a configured stall at the specified test configuration.
3) Set engine power to flight idle.
4) Slow the aircraft to approximately 10 kts above stall speed.
5) Pitch airplane to decelerate at a rate less than 1 knot per second.
6) Maintain wings level, zero yaw rate.
7) Record indicated airspeed at key events such as stall warning, buffet, pitch down, yoke reaches full aft stop, minimum full aft stop speed, speed two seconds after full aft stop, etc.
8) Recover aircraft from stall at first indication of stall: uncontrolled downward pitch or yoke reaches aft stop for 2 seconds. Additionally, recover if bank angle exceeds 15 degrees or a significant yaw rate develops.

For intentional stalls above 5000' AGL, the aircrew followed the modified stall recovery procedure below:

1) Attitude – Pitch nose down to reduce the angle of attack below stall value
2) Wings – Level
3) Sideslip – Center ball
4) Power – As required
5) Attitude – Return to horizon
6) Gear – Up (when rate of descent breaks)
7) Airspeed – Return to trim speed
8) Flaps – Up

APPENDIX C – DATA ANALYSIS

DATA REQUIREMENTS

Table C1 describes the data that were collected for each FTT.

Table C1. Data Collected.

Name	Platform	Source	Units	FTTs
Instrument Correction	DAS C-12	Handheld Data	feet	Ground Calibration
Instrument Correction	Non-DAS C-12	Handheld Data	feet	Ground Calibration
Indicated Airspeed	DAS C-12	Handheld Data, DAS	knots	Stall Tower Flyby
Indicated Altitude	DAS C-12	Handheld Data, DAS	feet	Stall Tower Flyby
Aircraft Total Weight	DAS C-12	Handheld Data, DAS	pounds	Stall Angry Silv
Fuel Weight	DAS C-12	Handheld Data, DAS	pounds	Stall Angry Silv
Indicated Airspeed	Non-DAS C-12	Handheld Data	knots	Stall
Indicated Altitude	Non-DAS C-12	Handheld Data	feet	Stall
Aircraft Total Weight	Non-DAS C-12	Handheld Data	pounds	Stall
Fuel Weight	Non-DAS C-12	Handheld Data	pounds	Stall
Indicated-Corrected Static Pressure (P_s)	DAS C-12	DAS		Stall Angry Silv
Indicated-Corrected Total Pressure (P_T)	DAS C-12	DAS		Stall Angry Silv
Total Air Temperature	DAS C-12	DAS		Stall
Radar Altimeter Reading	DAS C-12	DAS		Stall
Engine Torque	DAS C-12	DAS		Stall
Indicated Angle of Attack (α_i)	DAS C-12	DAS		Stall Angry Silv
Propeller RPM	DAS C-12	DAS		Stall
Mach Number	DAS C-12	DAS		Stall
Elevator Position	DAS C-12	DAS		Stall
Yoke Position	DAS C-12	DAS		Stall
Normal Load Factor	DAS C-12	DAS		Stall
GPS Time	DAS C-12	GAINR Lite		Stall
Geometric Altitude (h_g)	DAS C-12	GAINR Lite		Stall Angry Silv
Vertical Velocity Down (v_D)	DAS C-12	GAINR Lite		Stall Angry Silv
Roll Angle (Φ)	DAS C-12	DAS		Angry Silv
Pitch Angle (Θ)	DAS C-12	DAS		Angry Silv

Name	Platform	Source	Units	FTTs
Yaw Angle (Ψ)	DAS C-12	DAS		Angry Silv
North Velocity (v_N)	DAS C-12	GAINR Lite		Angry Silv
East Velocity (v_E)	DAS C-12	GAINR Lite		Angry Silv
Indicated Angle of Sideslip (β_i)	DAS C-12	DAS		Angry Silv
Instrument Corrected Temperature (T_{ic})	DAS C-12	DAS		Angry Silv Tower Flyby
Ambient Pressure	N/A	Weather Balloon		Angry Silv
Ambient Temperature	N/A	Weather Balloon		Angry Silv
Time	DAS C-12	Handheld Data		Tower Flyby
Theodolite Measurement	Tower	Handheld Data		Tower Flyby
Theodolite Pressure Altitude	Tower	Handheld Data		Tower Flyby
Theodolite Ambient Temperature	Tower	Handheld Data		Tower Flyby
Time	Tower	Handheld Data		Tower Flyby

AIRSPEED DATA ANALYSIS

Instrument-Corrected Airspeed at Stall

The test team calibrated the air data system on the ground prior to the start of testing using a TTU-205 calibrated pressure source attached to the total and static pressure ports. The TTU-205 simulated the total and static pressure at a variety of altitudes and airspeeds. A Druck™ Precision Pressure Monitor (PPM) was connected in series between the TTU-205 and the aircraft ports and provide a truth source of the altitude and airspeed. The difference between the truth source's altitude/airspeed and the indicated altitude/airspeed was recorded by hand and used as an instrument correction (ΔV_{ic}). This, combined with the indicated airspeed (V_i) read from the aircraft in flight, was used to determine the instrument-corrected airspeed on the non-DAS aircraft.

$$V_{ic} = V_i + \Delta V_{ic}$$

The DAS aircraft recorded the production total and static pressure, as well as the boom total pressure. Boom static pressure was unreliable and therefore not used. The DAS and production (ADC 1) instrument-corrected airspeed (V_{ic}) were determined by the following equation:

$$V_{ic} = \sqrt{\left(\frac{1}{\rho_{SL}}\right) 7 P_{SL} \left(\left(\frac{P_t - P_s}{P_{SL}} + 1 \right)^{\frac{2}{7}} - 1 \right)}$$

Where:

$P_{SL} = 2116.2\ \text{lb/ft}^2$ is the atmospheric pressure at sea level
P_s is the static pressure measured by the production system
P_t is the total pressure measured by the production system or boom
$\rho_{SL} = 0.0023769\ \text{slugs/ft}^3$ is the standard sea level density

The total boom pressure and production static pressure were used to determine the DAS V_{ic}. The production total and static pressures were used to determine the production (ADC 1) V_{ic}.

Calibrated Airspeed at Stall

The airspeed position error, ΔV_{pc}, was computed using the JMOSS algorithm applied to the stall data. This algorithm is provided in the digital appendix (Appendix G). The calibrated airspeed V_c can be obtained from the instrument-corrected airspeed and the position error by using the following equation:

$$V_c = V_{ic} + \Delta V_{pc}$$

The DAS instrument-corrected airspeed and JMOSS ΔV_{pc} were used to generate a calibrated stall speed for each stall maneuver.

The production system ΔV_{pc} was determined by subtracting the production system V_{ic} from the calculated V_c.

Generate Stall Speed Table

In order to generate flight manual Figures 6-1 and 6-2, the equivalent airspeed V_e was also required. The f-factor, used to convert calibrated to equivalent airspeeds, was approximately 1 across the C-12 operating envelope; therefore, $V_c = V_e$.

The true airspeed (V_t) is related to the equivalent airspeed (V_e) by the following equation:

$$V_e = V_t \sqrt{\frac{\rho}{\rho_{SL}}}$$

This relationship allows the lift coefficient at stall, $C_{L_{max}}$ to be determined by the following equation.

$$C_{L_{max}} = \frac{nW}{\frac{1}{2}\rho V_t^2 S} = \frac{nW}{\frac{1}{2}\rho_{SL} V_{e_{stall}}^2 S}$$

Where:

n is the load factor
W is the aircraft weight
S is the planform area of the aircraft, 303 ft^2 per the flight manual (reference 7)

The load factor, n, was found from the bank angle, ϕ, assuming that the aircraft is flying level.

$$n = \frac{1}{\cos \phi}$$

The $C_{L_{max}}$ was calculated for each stall. All stalls were characterized by a g-break, therefore the $C_{L_{max}}$ for each configuration of stall was averaged to determine a $C_{L_{max}}$. All of the clean stall $C_{L_{max}}$ values were averaged to determine a single, clean configuration value. This was also done to determine an approach configuration $C_{L_{max}}$ value and a landing configuration $C_{L_{max}}$ value.

These three $C_{L_{max}}$ values were used to determine stall speeds ($V_{c_{stall}}$) at the weights and bank angles required for Figures 6-1 and 6-2 in the flight manual by using the following model:

$$V_{c_{stall}} = \sqrt{\frac{nW}{\frac{1}{2}\rho_{SL} C_{L_{max}} S}}$$

Since the flight manual must match production representative airspeeds, the production system position error correction ΔV_{pc}, calculated in the section above was used. An equation to estimate ΔV_{pc} as a function of weight was calculated for each aircraft configuration. The ΔV_{pc} is plotted against aircraft gross weight for each configuration figures D1, D2, and D3 in Appendix D. The equation to calculate ΔV_{pc} is on each figure. These equations were applied to the calibrated airspeeds found above to determine the production-representative instrument-corrected stall airspeeds.

These methods are in line with *Pitot-Statics and the Standard Atmosphere* (reference 16).

Difference Between DAS and Non-DAS Indicated Airspeed at Stall

Indicated Airspeed (V_i) and indicated altitude (H_i) were read from the non-DAS aircraft's ADC 1. An instrument correction (ΔV_{ic}, ΔH_{ic}) was determined during ground testing. These two parameters were used to determine the instrument-corrected airspeed and altitude for the non-DAS aircraft.

$$V_{ic} = V_i + \Delta V_{ic}$$

$$H_{ic} = H_i + \Delta H_{ic}$$

The DAS aircraft production system instrument-corrected airspeeds were computed to compare production systems between the two aircraft using the following equation:

$$V_{ic} = \sqrt{\left(\frac{1}{\rho_{SL}}\right) 7 P_{SL} \left(\left(\frac{P_t - P_s}{P_{SL}} + 1 \right)^{\frac{2}{7}} - 1 \right)}$$

Where:

$P_{SL} = 2116.2\ \mathrm{lb/ft^2}$ is the atmospheric pressure at sea level
P_s is the static pressure measured by the production system
P_t is the total pressure measured by the production system
$\rho_{SL} = 0.0023769\ \mathrm{slugs/ft^3}$ is the standard sea level density

Non-DAS stall speeds were spot checked against the data set of stall speeds assuming normal distribution of DAS stall speeds. Frequencies of DAS stall speeds were plotted with a normal curve superimposed, and individual non-DAS stall events were scatter-plotted.

STATIC POSITION ERROR DETERMINATION

The static position error was determined using a customer-provided script available in the Digital Data Appendix, which used data from the Tower Flyby, "Angry Silv" maneuver, and weather balloon to determine SPE using the Tower Flyby, Survey, and JMOSS algorithms. This Appendix discusses methods of determining SPE.

Tower Flyby

Tower Flyby FTT

The tower flyby FTT provided low altitude test data at subsonic airspeeds. The aircraft flew down the tower flyby line at approximately 200 feet AGL, maintaining level flight and constant velocity. Abeam the tower, the aircrew recorded indicated altitude, indicated velocity, vertical velocity, fuel, and time. At the same time, a test team member in the flyby tower recorded geometric aircraft height using a theodolite, as well as the ambient pressure and ambient temperature in the tower. By comparing pressure altitude in the aircraft to pressure altitude calculated using geometric aircraft height from the tower, the test team determined a pressure error coefficient.

Tower Flyby Data Analysis

The tower flyby data reduction was performed by comparing the altitude readings of the test aircraft to the aircraft's altitude as read from a theodolite using the similar triangles method.

$$\Delta H = Theodolite\ Measurement * 31.4$$

This change in geometric altitude was used to solve for the altitude correction ΔH_c.

$$\Delta H_c = \Delta H \frac{T_{std}}{T_{test}}$$

T_{test} was the ambient temperature measured in the fly-by tower and T_{std} was the standard day temperature at the pressure altitude measured in the tower. The truth pressure altitude of the aircraft can be calculated.

$$H_c = H_{c_{tower}} + \Delta H_c$$

The instrument corrected airspeed and altitude of the aircraft were calculated by adding instrument corrections to the indicated values from the aircraft. Using these instrument corrected values, the test team solved for ΔH_{pc} (position corrected altitude) for a given instrument airspeed.

$$\Delta H_{pc} = H_c - H_{ic}$$

Finally, the test team solved for the position error ΔP_p from the static and ambient pressure.

$$P_s = P_{SL}(1 - 6.87559 * 10^{-6} H_{ic})^{5.2559}$$

$$P_a = P_{SL}(1 - 6.87559 * 10^{-6} H_c)^{5.2559}$$

$$\Delta P_p = P_s - P_a$$

And the static position error was found using $\Delta P_p / P_s$.

Survey Method

Survey Method FTT

In this technique, a weather balloon capable of measuring ambient temperature, pressure altitude, and ambient pressure was launched into the local air mass. The balloon measurements of ambient pressure were then directly used to compute SPE. The survey method assumes constant atmospheric properties between the balloon and the area where the experimental aircraft collects its data. This assumption also limits the test window because the truth data needed for calibration is only available and/or valid for a limited time and geographic location.

Survey Method Data Analysis

The instrument corrected altitude H_{ic} was used to determine to static pressure P_s using the following equation.

$$P_s = P_{SL}(1 - 6.87559 * 10^{-6} H_{ic})^{5.2559}$$

The geometric altitude h of the aircraft was determined via TSPI vertical position information. The weather balloon(s) data were used to determine the ambient pressure P_a at that same geometric altitude.

This allowed the test team to derive directly the static position error, comparing the ambient pressure (balloon information) with the static pressure measured by the aircraft.

$$\Delta P_p = P_s - P_a$$

From there, the static position error ratio $\Delta Pp/Ps$ was calculated directly.

JMOSS Method

JMOSS was based on a statistical analysis of continuous flight data, with a model of the unknown SPE created based on classical curve fitting techniques. It was successfully demonstrated on a T-38 in the Have SPEED program (reference 12), and the test team used the version given in the Digital Data Appendix (Appendix G) to determine the SPE on the C-12. As flight data were analyzed, a model of the unknowns (static position error being the unknown of interest) was created based on classical curve fittings. As the model was built, a statistical analysis of the relevancy of each possible curve fitting was executed, keeping the best fit as a local solution.

Figure C1 depicts a flow chart of the process associated with the JMOSS statistical method and data reduction technique. For each set of test data, a set of inputs (shown on the far left of the figure) were taken from the test aircraft. GPS data was collected from the GAINR Lite TSPI system and air data system (ADS) and inertial measurements (IMU) were collected from aircraft via the DAS.

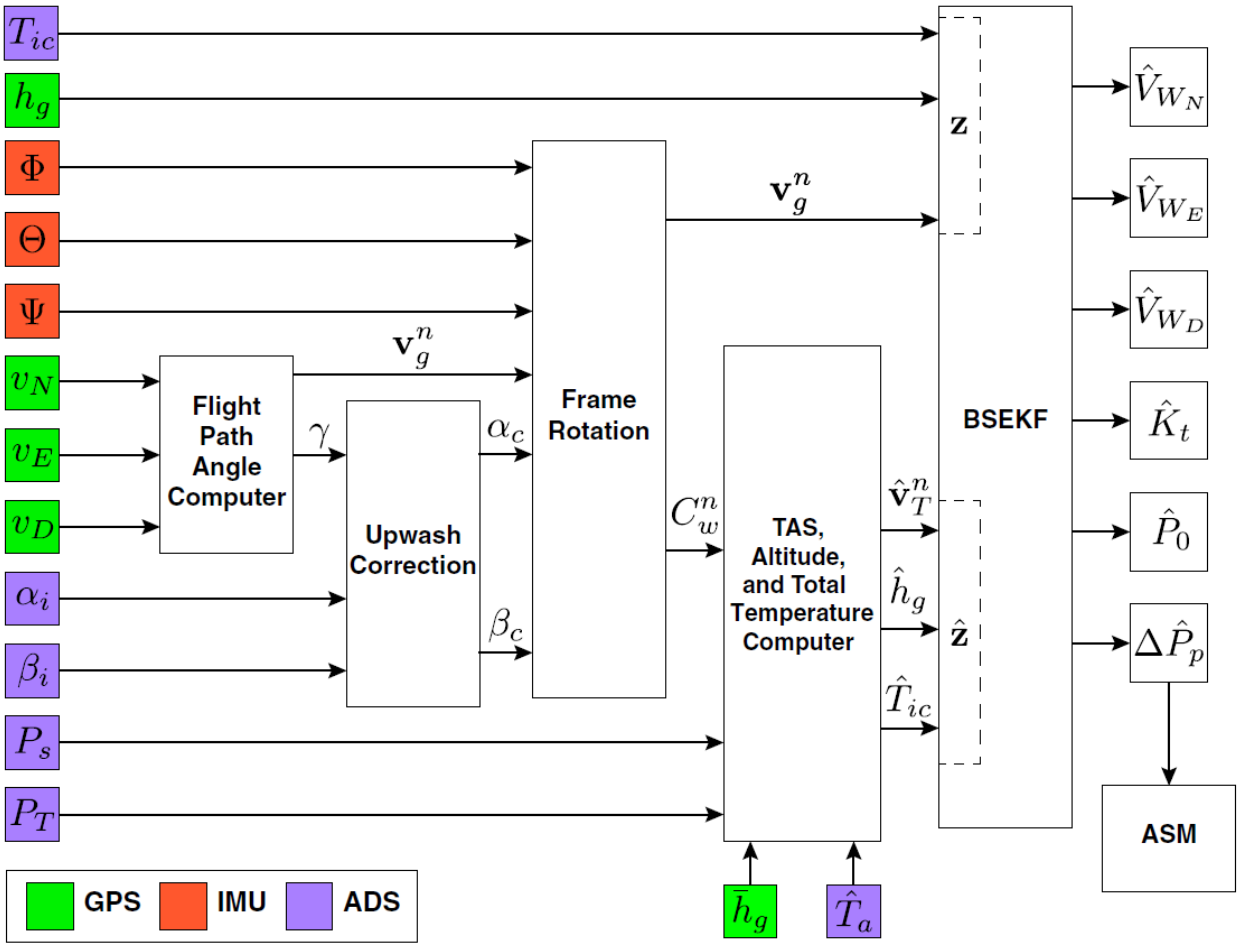

Figure C1. Flow Chart Depicting the JMOSS Data Reduction Algorithm

JMOSS first ran a Backwards-Smoothing Extended Kalman Filter (BSEKF) on the continuous data, represented by the 12 parameters on the left side of Figure C1. It produced continuous estimates of six variables of interest on the right of Figure C1. The BSEKF produces estimates of the North wind component ($\hat{V}_{W_N}$), East wind component ($\hat{V}_{W_E}$), downward wind component ($\hat{V}_{W_D}$), SPE ($\Delta\hat{P}_p$), temperature correction factor ($\hat{K}_t$), and a pressure bias ($\hat{P}_0$) for each time step of the input data. The SPE was the parameter of interest for this program and was used to generate a GLM using methods described in the next section.

STATISTICAL ANALYSIS

The customer employed the JMOSS algorithm in data analysis to generate SPE. The JMOSS data was processed using SPSS Statistics to construct the model of SPE by Mach number and angle of attack as follows:

$$SPE = \beta_0 + \beta_1 * Mach + \beta_2 * AoA + \beta_3 * Mach^2 + \beta_4 * AoA^2 + \beta_5 * Mach * AoA;$$

This returned a table of estimated coefficients. The function also returned standard error, t-statistics, and p-values for each coefficient, as well as degrees of freedom, dispersion and F-statistic with p-value for the model. Statistical significance was measured by the reported p-values: lower p-values translating to higher confidence. Effect sizes were assessed using the coefficient of determination ($r^2 = 1 - \frac{SS_{residual}}{SS_{total}}$)

for the full model, and partial Eta-squared (Partial $\eta^2 = \frac{SS_{effect}}{SS_{effect}+SS_{error}}$) for coefficients. Partial η^2 can also be described as the ratio of variance explained in the dependent variable by a predictor. For the initial model, the test team observed a low $r^2 = 0.124$ with partial Eta-square as low as $\eta^2 = 0.007$. The decision was made to explore the main effects of combinations of the variables in different combinations iteratively, to increase the power of the coefficient of determination, and report an analysis of covariance (ANCOVA) as well as the generalized linear model (GLM). Type III sum of squares were used to adjusted for all effects. Consequently, the standalone variable of AOA was omitted from the reported GLM. Ultimately, the model was specified as:

$$SPE = \beta_1 * \ Mach \ + \beta_2 * Mach * AoA; + \beta_3 * AoA^2$$

Results of evaluation of the assumptions of normality of sampling distributions, linearity, homogeneity of variance, homogeneity of regression, and reliability of covariates were satisfactory. A sample size of N=226,405 DAS datapoints from "Angry Silv" maneuvers was used, with 3.2% excluded. Each of the included covariates exhibited statistically significant main effects, in all iterations of the model. The final model was judged to be strongest due to the $r^2 = 0.644$. The strength of the relationship between SPE and Mach number was particularly strong at $\eta^2 = 0.632$. The other effects were much weaker. The full SPSS analysis of covariates and residuals is included in the digital appendix.

Mean squared error was reported for the comparisons JMOSS, balloons, and tower flyby SPE reporting methods. MSE is computed as follows:

$$MSE = \frac{1}{n}\sum_{i=1}^{n}\left(Y_i - \hat{Y}_i\right)^2$$

APPENDIX D – SUPPLEMENTAL DATA

Tables D1, D2, and D3 present the stall data for all stalls performed in the clean, powered-approach, and landing configurations, respectively, in the DAS aircraft. Figures D1, D2, and D3 plotted the production ΔV_{pc} against aircraft gross weight for each configuration. The equation to calculate ΔV_{pc} is on each figure. Table D4 shows the stall data for the Non-DAS aircraft. Figure D4 shows an enlarged version of the recommended flight manual stall update chart. The details on how these data were calculated was described in Appendix C.

Table D1. Cruise Configuration Stall Data

Pressure Altitude (ft)	Aircraft Gross Weight (pounds)	Angle of Bank (degs)	Static Pressure, P_s (psi)	Total Boom Pressure, P_t (psi)	Total Production Pressure, P_t (psi)	DAS Instrument Corrected Airspeed, V_{ic} (knots)	JMOSS DAS Position Correction, ΔV_{pc} (knots)	Calibrated Airspeed, V_c (knots)	Lift Coefficient, $C_{L_{max}}$ (no units)	Production Instrument Corrected Airspeed, V_{ic} (knots)	Production Position Correction, ΔV_{pc} (knots)
8684	10633	1.1	10.63	10.84	10.84	93.13	-4.07	89.06	1.31	93.46	-4.40
8759	10726	-2.8	10.61	10.80	10.80	91.55	-0.95	90.60	1.28	91.52	-0.91
8488	10924	-3.9	10.71	10.92	10.92	92.84	-1.43	91.41	1.28	92.84	-1.43
19655	10925	-7.0	6.85	7.06	7.06	93.94	-4.41	89.54	1.34	94.02	-4.48
8843	11002	0.7	10.56	10.78	10.78	95.30	-4.90	90.40	1.31	95.61	-5.21
19635	11048	14.6	6.87	7.07	7.07	93.81	-4.01	89.81	1.38	93.58	-3.77
8629	11075	9.8	10.66	10.87	10.87	93.92	-2.92	91.00	1.32	94.26	-3.26
8594	11107	-7.8	10.67	10.88	10.88	93.22	-0.54	92.67	1.27	93.28	-0.61
19401	11112	0.3	6.93	7.14	7.14	93.08	0.23	93.31	1.24	92.86	0.45
13724	11142	7.7	8.73	8.94	8.94	93.05	-3.23	89.82	1.36	93.23	-3.40
19664	11157	9.1	6.85	7.05	7.05	92.02	-5.07	86.95	1.46	92.37	-5.41
8660	11204	1.0	10.64	10.86	10.86	94.73	-3.09	91.64	1.30	94.74	-3.11
19613	11259	-0.2	6.87	7.08	7.08	94.92	-1.21	93.70	1.25	94.85	-1.15
8634	11280	-6.9	10.66	10.87	10.87	93.46	-2.15	91.31	1.33	93.48	-2.17
19594	11280	-3.8	6.87	7.09	7.08	95.29	-4.79	90.49	1.35	95.08	-4.59
13831	11329	6.1	8.70	8.91	8.91	95.19	-2.93	92.26	1.30	95.04	-2.78
13735	11356	2.7	8.73	8.94	8.94	94.58	-2.87	91.71	1.32	94.55	-2.84
8548	11373	-4.0	10.69	10.90	10.90	93.41	-1.70	91.71	1.32	93.03	-1.32
19520	11427	4.6	6.89	7.10	7.10	94.78	-3.33	91.45	1.34	94.14	-2.69
19514	11489	-8.1	6.89	7.11	7.11	96.28	-4.21	92.06	1.33	96.09	-4.03
8376	11510	-5.6	10.76	10.97	10.97	94.59	-0.11	94.48	1.26	94.67	-0.18
13964	11585	0.1	8.65	8.87	8.87	97.57	-3.72	93.84	1.28	97.30	-3.46
19452	11611	4.9	6.91	7.13	7.13	97.09	-3.67	93.42	1.30	97.33	-3.91
8562	11717	-8.0	10.69	10.90	10.91	95.57	-0.90	94.67	1.29	95.75	-1.08
13933	11719	-9.3	8.66	8.88	8.88	98.26	-2.89	95.37	1.27	98.01	-2.64
8370	11724	8.5	10.77	10.99	10.99	96.95	-2.66	94.29	1.30	96.57	-2.28
19550	11793	7.6	6.88	7.11	7.11	97.44	-3.21	94.23	1.31	97.59	-3.36
13994	11796	10.0	8.64	8.86	8.86	95.69	-5.66	90.03	1.44	95.46	-5.43
8531	11803	12.8	10.69	10.93	10.93	98.68	-2.86	95.82	1.28	99.24	-3.42
8384	11912	3.9	10.76	10.98	10.98	96.68	-2.35	94.34	1.31	96.89	-2.55
8304	11943	-5.0	10.79	11.02	11.02	98.89	-2.97	95.92	1.27	98.82	-2.90
8465	11972	-3.7	10.73	10.96	10.96	98.07	-1.84	96.23	1.26	98.22	-1.99
19630	12012	0.9	6.86	7.09	3.48	98.57	-6.93	91.63	1.39	98.21	-6.58
13923	12065	-4.2	8.67	8.89	4.37	96.57	-2.48	94.09	1.33	96.47	-2.38
8263	12129	-0.6	10.81	11.06	11.06	101.56	-2.68	98.89	1.21	101.54	-2.66
8684	10633	1.1	10.63	10.84	10.84	93.13	-4.07	89.06	1.31	93.46	-4.40

Table D2. Powered Approach Configuration Stall Data

Pressure Altitude (ft)	Aircraft Gross Weight (pounds)	Angle of Bank (degs)	Static Pressure, P_s (psi)	Total Boom Pressure, P_t (psi)	Total Production Pressure, P_t (psi)	DAS Instrument Corrected Airspeed, V_{ic} (knots)	JMOSS DAS Position Correction, ΔV_{pc} (knots)	Calibrated Airspeed, V_c (knots)	Lift Coefficient, $C_{L_{max}}$ (no units)	Production Instrument Corrected Airspeed, V_{ic} (knots)	Production Position Correction, ΔV_{pc} (knots)
8354	10600	1.3	10.78	10.94	10.94	82.62	-2.79	79.83	1.62	82.67	-2.84
8867	10702	-0.9	10.56	10.72	10.71	79.81	-0.48	79.34	1.66	78.38	0.96
13988	10778	-5.0	8.64	8.80	8.80	82.17	-1.20	80.97	1.61	81.64	-0.67
8673	10901	-0.4	10.64	10.80	10.79	81.25	0.00	81.25	1.61	79.53	1.73
13908	10920	-1.0	8.67	8.82	8.82	80.60	-0.14	80.46	1.64	79.75	0.71
19420	11014	1.0	6.93	7.08	7.08	81.84	-2.14	79.70	1.69	80.50	-0.80
14179	11055	-3.2	8.58	8.74	8.74	83.00	-1.09	81.90	1.61	82.07	-0.16
19232	11084	-0.1	6.98	7.14	7.13	82.62	0.94	83.56	1.55	81.05	2.51
8541	11085	0.0	10.70	10.85	10.85	81.46	1.46	82.92	1.57	79.78	3.14
13782	11108	-5.8	8.71	8.88	8.88	85.95	-4.01	81.93	1.62	85.65	-3.71
8417	11181	-5.7	10.75	10.91	10.91	83.12	-1.26	81.86	1.63	82.14	-0.28
13498	11222	-0.5	8.81	8.98	8.97	82.91	-1.93	80.97	1.67	81.93	-0.95
19319	11232	-0.4	6.95	7.11	7.11	82.11	-0.44	81.66	1.64	80.91	0.75
19849	11248	-2.3	6.80	6.96	6.96	82.51	-3.89	78.62	1.78	81.36	-2.74
8535	11256	-1.0	10.70	10.86	10.85	82.17	-1.80	80.37	1.70	80.84	-0.47
13676	11295	-1.4	8.75	8.91	8.91	83.38	-1.98	81.40	1.66	81.76	-0.36
14006	11318	-3.1	8.63	8.81	8.80	85.60	-2.97	82.63	1.62	84.43	-1.80
8251	11345	-3.8	10.81	10.99	10.98	86.37	-3.84	82.53	1.63	85.57	-3.04
19421	11402	-3.0	6.92	7.09	7.08	84.91	-2.03	82.88	1.62	83.73	-0.85
19430	11460	0.3	6.92	7.09	7.08	83.34	-3.00	80.34	1.73	81.73	-1.38
8467	11482	1.8	10.73	10.89	10.88	83.16	0.58	83.74	1.60	81.94	1.79
14164	11506	-3.9	8.59	8.76	8.76	84.47	-1.84	82.63	1.65	83.74	-1.11
19232	11582	-2.1	6.98	7.15	7.15	85.61	-3.26	82.35	1.67	85.04	-2.69
8438	11683	-7.6	10.74	10.91	10.90	84.47	-1.78	82.69	1.68	83.94	-1.25
8801	11683	1.2	10.59	10.76	10.75	85.11	-0.01	85.10	1.57	83.41	1.69
19334	11765	0.3	6.95	7.13	7.13	87.38	-3.81	83.56	1.64	87.25	-3.68
13670	11766	-4.5	8.75	8.93	8.93	85.45	-6.04	79.42	1.82	85.17	-5.76
19748	11909	-1.1	6.83	7.00	7.00	86.75	-2.89	83.85	1.65	85.15	-1.30
13497	11957	0.6	8.81	8.98	8.98	85.32	-5.26	80.06	1.82	83.89	-3.83
19186	11981	0.4	7.00	7.19	7.18	89.71	-5.97	83.74	1.67	89.48	-5.74
19656	11992	-2.2	6.85	7.03	7.03	87.14	-2.98	84.16	1.65	85.47	-1.30
13713	12029	-1.6	8.74	8.91	8.91	86.89	-2.12	84.77	1.63	85.25	-0.47
8885	12048	-0.9	10.56	10.73	10.73	86.39	-0.85	85.54	1.61	84.75	0.80
8601	12073	0.5	10.67	10.85	10.84	87.37	-1.81	85.56	1.61	85.44	0.12
8867	12093	-0.7	10.57	10.74	10.73	84.97	-0.53	84.44	1.65	83.23	1.20
8475	12115	-1.6	10.72	10.90	10.90	87.62	-1.95	85.66	1.61	86.13	-0.47

Table D3. Landing Configuration Stall Data

Pressure Altitude (ft)	Aircraft Gross Weight (pounds)	Angle of Bank (degs)	Static Pressure, P_s (psi)	Total Boom Pressure, P_t (psi)	Total Production Pressure, P_t (psi)	DAS Instrument Corrected Airspeed, V_{ic} (knots)	JMOSS DAS Position Correction, ΔV_{pc} (knots)	Calibrated Airspeed, V_c (knots)	Lift Coefficient, $C_{L_{max}}$ (no units)	Production Instrument Corrected Airspeed, V_{ic} (knots)	Production Position Correction, ΔV_{pc} (knots)
8812	10572	1.6	10.58	10.71	10.70	72.54	-2.99	69.54	2.13	70.99	-1.45
8674	10675	1.8	10.64	10.76	10.75	70.32	0.31	70.63	2.09	68.42	2.21
13983	10746	2.4	8.63	8.77	8.76	77.30	-4.05	73.25	1.95	75.93	-2.68
8797	10875	1.2	10.59	10.71	10.70	71.78	2.37	74.15	1.93	69.47	4.68
13974	10887	6.1	8.65	8.77	8.76	72.14	0.00	72.13	2.05	70.60	1.54
13797	11026	4.4	8.71	8.83	8.83	73.05	-1.02	72.03	2.08	71.98	0.05
8747	11058	0.7	10.61	10.73	10.73	71.79	4.41	76.20	1.86	69.67	6.54
14016	11072	2.6	8.63	8.75	8.75	71.86	-0.89	70.98	2.14	69.95	1.03
13765	11147	1.0	8.72	8.85	8.84	74.11	-1.54	72.57	2.06	72.30	0.27
8360	11150	6.4	10.77	10.90	10.89	72.04	0.51	72.55	2.08	70.24	2.30
13683	11184	6.0	8.75	8.87	8.87	72.57	-1.39	71.17	2.16	70.85	0.33
19134	11200	4.2	7.01	7.13	7.13	72.74	1.22	73.96	2.00	71.30	2.66
8241	11223	0.6	10.82	10.94	10.93	72.30	0.27	72.57	2.08	70.02	2.54
13773	11260	7.6	8.71	8.85	8.84	77.47	-4.68	72.80	2.09	74.94	-2.15
13748	11287	1.2	8.72	8.85	8.84	72.80	-2.00	70.80	2.20	71.32	-0.52
19199	11365	3.2	6.99	7.12	7.11	73.67	0.85	74.53	2.00	72.44	2.09
14315	11468	2.1	8.53	8.66	8.65	73.95	-0.97	72.98	2.10	71.81	1.17
19305	11542	4.6	6.96	7.09	7.08	73.90	-0.39	73.51	2.09	72.74	0.77
8412	11652	6.6	10.75	10.87	10.87	72.09	1.00	73.09	2.14	70.98	2.11
8471	11653	6.4	10.70	10.86	10.85	80.36	-5.16	75.20	2.02	78.63	-3.42
13700	11721	1.2	8.74	8.87	8.86	75.22	-5.38	69.84	2.34	72.42	-2.59
19281	11724	2.1	6.96	7.10	7.09	74.65	-0.90	73.75	2.10	73.25	0.50
13904	11916	1.3	8.67	8.81	8.80	76.67	-6.09	70.57	2.33	74.30	-3.73
19301	11928	1.8	6.96	7.09	7.08	75.09	-2.16	72.94	2.19	73.15	-0.22
19624	11942	7.4	6.86	7.00	7.00	76.83	-4.36	72.47	2.24	75.12	-2.65
13952	11987	0.2	8.65	8.79	8.78	75.08	-1.94	73.14	2.18	72.97	0.18
8574	12170	0.1	10.68	10.82	10.81	76.30	-0.89	75.41	2.09	74.58	0.82
8214	12226	12.2	10.83	10.96	10.96	75.45	-1.13	74.32	2.21	73.90	0.42
8812	10572	1.6	10.58	10.71	10.70	72.54	-2.99	69.54	2.13	70.99	-1.45
8674	10675	1.8	10.64	10.76	10.75	70.32	0.31	70.63	2.09	68.42	2.21
13983	10746	2.4	8.63	8.77	8.76	77.30	-4.05	73.25	1.95	75.93	-2.68

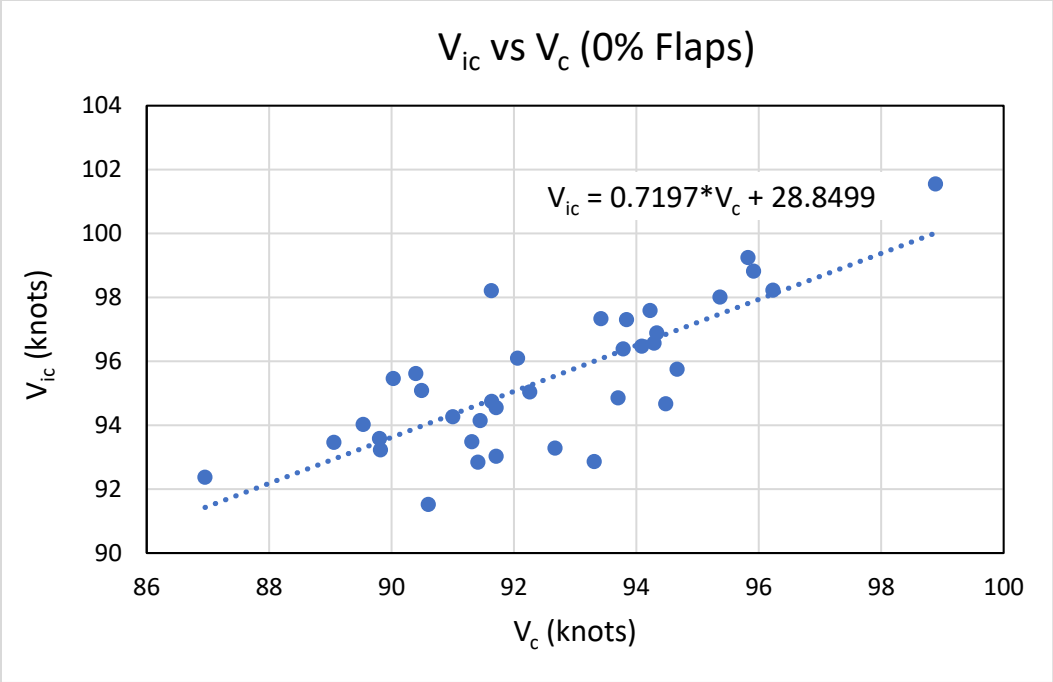

Figure D1. Production System Position Error Correction, Clean Configuration

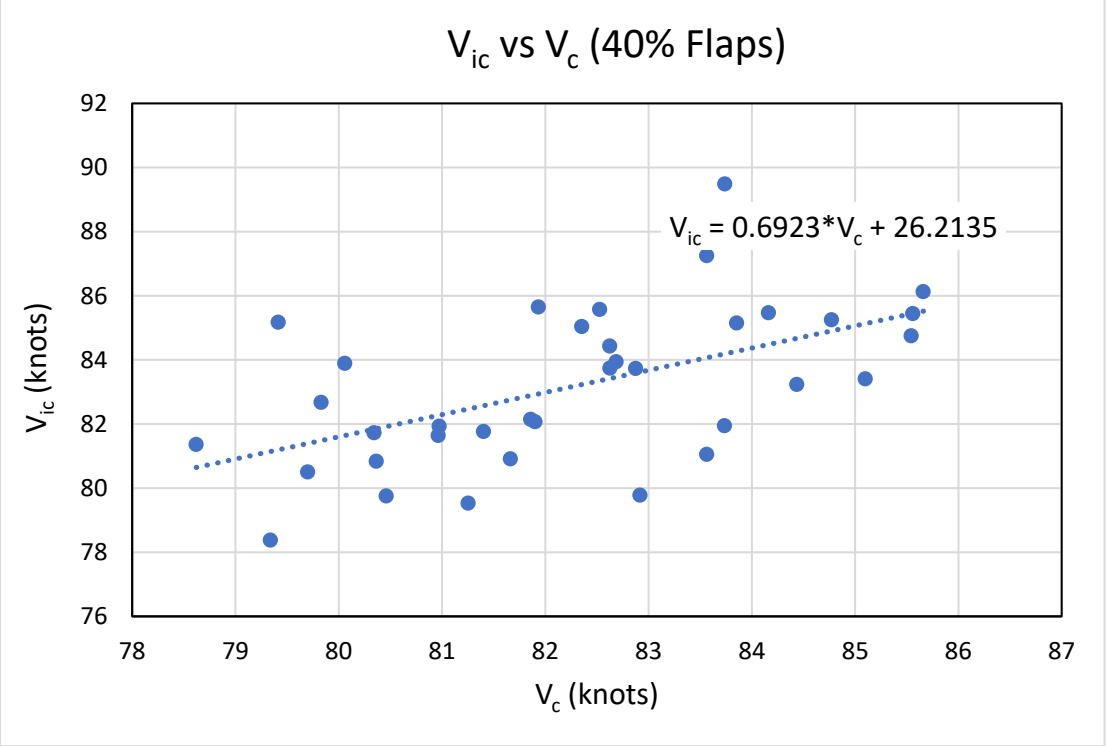

Figure D2. Production System Position Error Correction, Approach Configuration

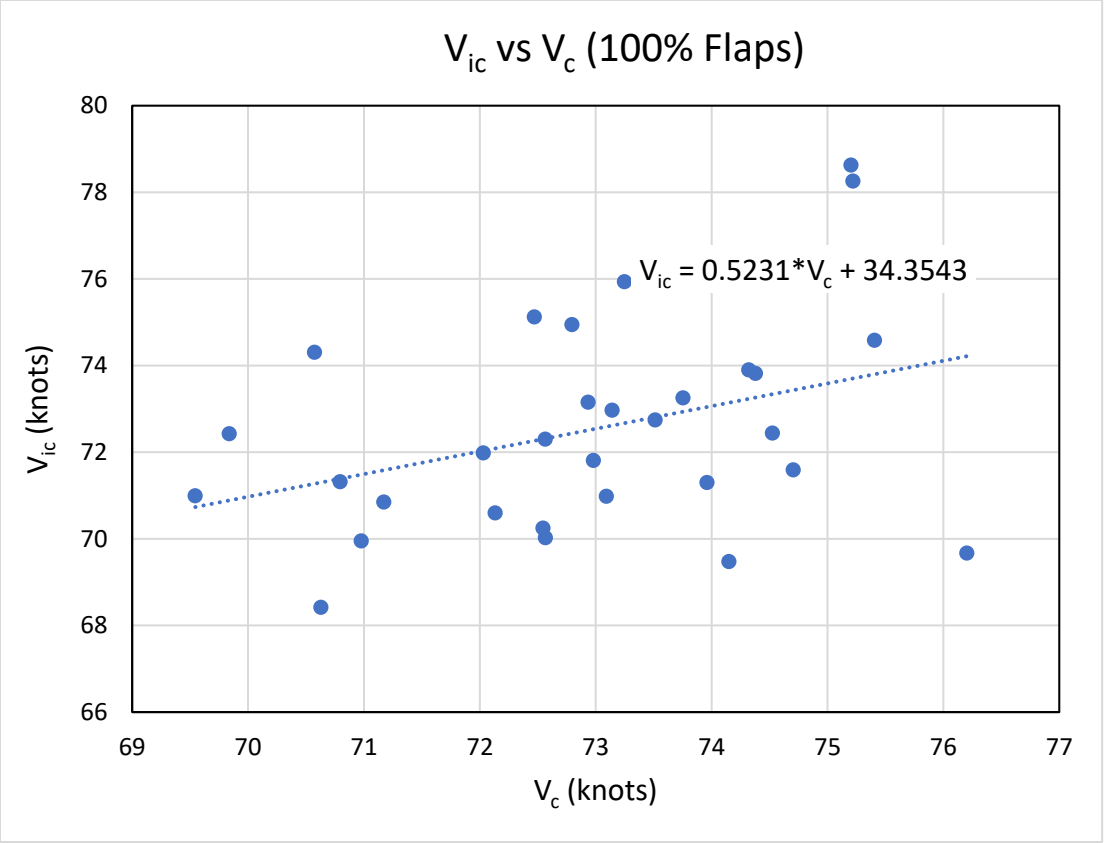

Figure D3. Production System Position Error Correction, Landing Configuration

Table D4. Non-DAS Stall Data

Configuration	Pressure Altitude (ft)	Aircraft Gross Weight (pounds)	Indicated Airspeed, V_i (knots)	Instrument Correction, ΔV_{ic} (knots)	Instrument Corrected Airspeed, V_{ic} (knots)
Clean	8520	10900	91	0.0	91.0
	8910	10980	91	0.0	91.0
	8700	11050	93	0.0	93.0
	8680	11590	95	0.0	95.0
	8590	11765	96	0.0	96.0
Approach	8640	10900	76	0.1	76.1
	8700	10955	77	0.1	77.1
	8770	11040	76	0.1	76.1
	8710	11590	80	0.0	80.0
	9000	11655	79	0.1	79.1
	8410	11660	80	0.1	80.1
Landing	8640	10870	70	0.1	70.1
	8890	10955	70	0.4	70.4
	8740	11000	71	0.2	71.2
	8560	11580	71	0.1	71.1
	8480	11580	71	0.0	71.0
	8700	11615	72	0.2	72.2

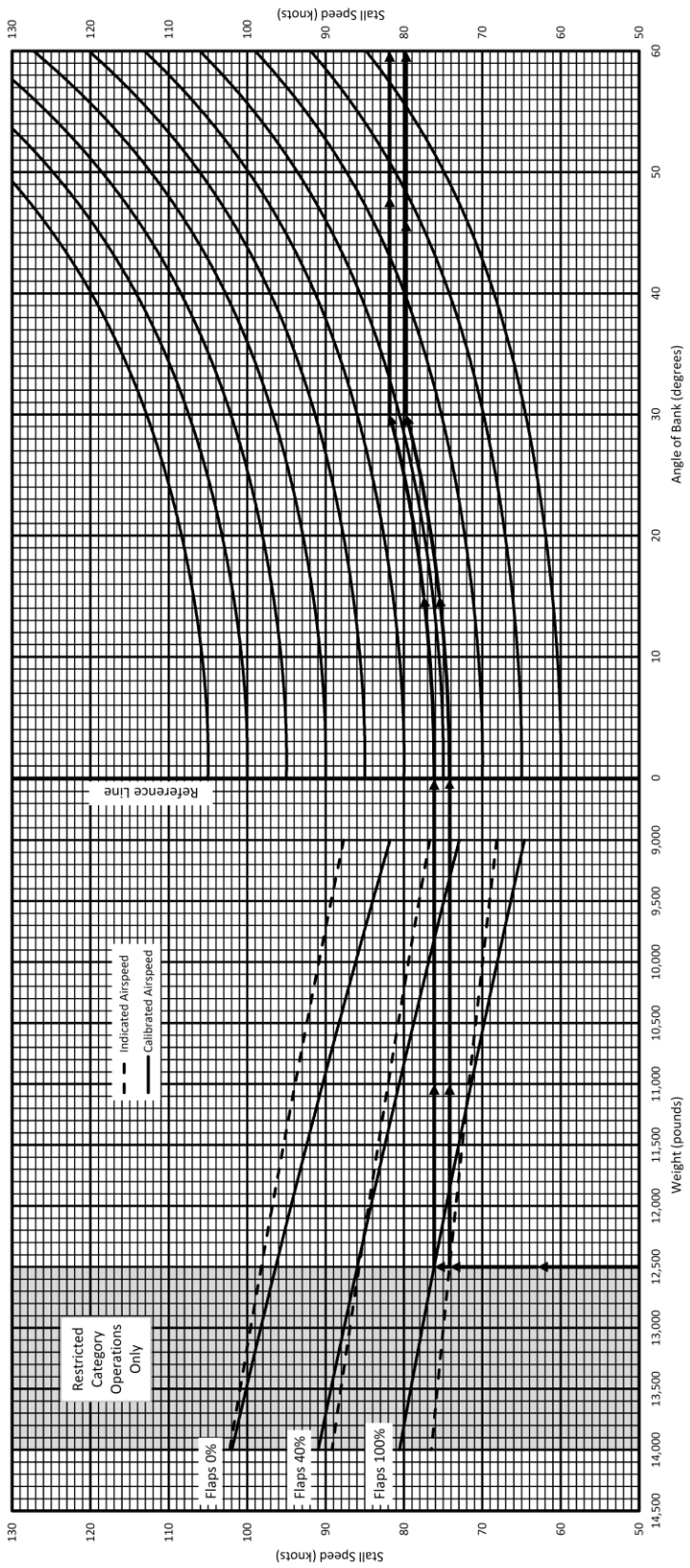

Figure D4. Proposed Flight Manual Stall Chart Update

Table D5. Tower Flyby Handheld Data

Indicated Airspeed, V_i (knots)	Indicated Altitude, H_i (feet)	Aircraft Indicated Temperature (°C)	Grid Reading	Tower Pressure Altitude, H_c (feet)	Tower Ambient Temperature (°C)	Fuel Weight (pounds)	Aircraft Gross Weight (pounds)
183	2460	23	7.5	2318	31.1	2700	12000
239	2480	23	6.75	2317	30.7	2700	12000
147	2440	24	6.75	2323	33.3	2500	12000
180	2270	15	5	2179	11.8	2200	11600
232	2340	21	6.3	2180	12.2	2125	11525
140	2260	21	5	2178	12.4	2100	11500
181	2300	16	6.25	2174	14.8	1525	10925
238	2320	17	5.5	2174	15.5	1500	10900
140	2290	16	6.3	2174	16	1400	10800

This page was intentionally left blank.

APPENDIX E – TEST CONDITION MATRIX

Table E1. Non-DAS Aircraft Test Condition Matrix

Test Maneuver	Configuration	Altitude Data Band (feet)	Airspeed (KIAS)	Weight Band	Flown	Comments
Stall	Clean	8,000 – 9,000 PA	1.5 Vstall - Vstall	10,500-11,100	3	Flaps Up, Gear Up, CG: 0-20%
				11,100-11,800	2	
	Approach		1.3 Vstall - Vstall	10,500-11,100	3	Flaps 40%, Gear Down, CG: 0-20%
				11,100-11,800	3	
	Landing			10,500-11,100	3	Flaps 100%, Gear Down, CG: 0-20%
				11,100-11,800	3	

Table E2. DAS Aircraft Test Condition Matrix

Test Maneuver	Configuration	Altitude Data Band (feet)	Airspeed (KIAS)	Weight Band	Roller Coaster / Turn Mach	Flown
Stall	Clean	8,000 – 20,000 PA	1.5 Vstall - Vstall	10,500-11,100	N/A	13
				11,100-11,800		14
				11,800-12,500		10
	Approach		1.3 Vstall - Vstall	10,500-11,100		10
				11,100-11,800		12
				11,800-12,500		10
	Landing			10,500-11,100		10
				11,100-11,800		12
				11,800-12,500		10
Tower Flyby	Clean	200-250 AGL	140	10,500-11,100		1
				11,100-11,800		1
				11,800-12,500		1
			180	10,500-11,100		1
				11,100-11,800		1
				11,800-12,500		1
			240 (or Vh)	10,500-11,100		1
				11,100-11,800		1
				11,800-12,500		1
The “Angry Silv" - Level Deceleration - Constant Mach Roller Coaster - Constant Mach Turn - Continuing Level Deceleration	Clean	8500 PA ± 500	220 (or Vh) - 1.5 Vstall	10,500-11,100	0.25M	1
				11,100-11,800		2
				11,800-12,500		1
				10,500-11,100	0.30M	1
				11,100-11,800		2
				11,800-12,500		1
				10,500-11,100	0.35M	1
				11,100-11,800		2
				11,800-12,500		1
				10,500-11,100	0.40M	1
				11,100-11,800		1
				11,800-12,500		1
		14000 PA ± 500		10,500-11,100	0.25M	1
				11,100-11,800		1
				11,800-12,500		1
				10,500-11,100	0.30M	1
				11,100-11,800		2
				11,800-12,500		1
				10,500-11,100	0.35M	1
				11,100-11,800		1
				11,800-12,500		1
				10,500-11,100	0.40M	1
				11,100-11,800		1
				11,800-12,500		1
		19500 PA ± 500		10,500-11,100	0.25M	1
				11,100-11,800		1
				11,800-12,500		1
				10,500-11,100	0.30M	1
				11,100-11,800		1
				11,800-12,500		1
				10,500-11,100	0.35M	1
				11,100-11,800		2
				11,800-12,500		1
				10,500-11,100	0.40M	1
				11,100-11,800		2
				11,800-12,500		1

APPENDIX F – LESSONS LEARNED

The following are lessons learned during the execution of Have EPIC DISCO:

- When additional assets are being used to collect data during a test flight and the test aircraft is delayed or canceled, it is important to call and let them know of the delays or cancelations as soon as possible to prevent unnecessary resource expenditures. Weather balloons were used to collect atmospheric data, but there were a few times that they weren't called until after the balloons were already launched or filled, making it too late to cancel launching the balloons.
- The ability to communicate as a team is key, which means that more than one person needs to have the contact information for all players involved in a test. If one person has the contact information for the weather balloons and they are unaware that the balloons need to be delayed, then the balloons will end up getting launched prematurely.
- It is just as important to have the aircraft in the right configuration and weight as it is for the test team to know what FTTs and test points they are attempting. Because the weight of the aircraft was part of the test plan, it was important to let the maintenance personnel know how much fuel to load into the aircraft prior to the next event. The best time for the test team to let them know how much fuel to put into the aircraft was when they returned from a sortie. However, follow up was required, especially for a non-standard fuel load. Additionally, it is important to specify tolerances on the fuel load given, especially when the weight or CG is near a limit.
- Flexibility was a useful tool that can only be available if proper planning has taken place. The test team was ready to change to different test conditions when turbulence, weather, airspace, etc. were uncooperative because they knew what data were still required. The ability to change the test points once airborne allowed the team to get all the desired test points from the test plan. If the team wasn't familiar with the data requirements, they would not have been able to collect all the data.
- Updating the test matrix at the end of each sortie allowed for efficient planning for follow on sorties. Knowing that the test matrix was correct at the beginning of each briefing prevented the team from wasting time trying to figure out if a test point had been completed or not, and helped the team know what the options were going to be if there were issues during the flight.
- The test plan had test points that were only attainable for a limited portion each flight. If you are able to identify these test points, you should try to get them early in the schedule. This allows multiple attempts to collect the data if you find out in post flight analysis that the planned data point was not obtained. This happened a few times as hand-held weight estimates were corrected with DAS fuel flow data. If you wait until the end of the fly window to try and get some of the more difficult points, you may be forced to choose which data points you will omit.
- It's better to ask for extra flight hours and not need them than to need them and not have them. In the second half of the TMP window, additional flight hours were needed due to early RTBs for maintenance issues. By recognizing the problem early, additional hours were approved.
- Ask questions early. A couple of flights were shortened so that corrective maintenance could be performed on the aircraft after an issue was observed airborne. After the third occurrence, it was determined that it would be ok to continue with the flight and that there was no need to RTB early because of it. By not asking the questions sooner, the number of sorties was increased unnecessarily. Receiving this guidance when the issue first appeared would have increased test efficiency.
- Seek out ways to reduce the cost of your test project by "piggy backing" off of other missions. One member of the test team was able to complete the crew-solo training requirements while

flying as a chase aircraft for a different test. This reduced spending for training, potentially allowing more flight hours.

- Equipment calibration is extremely important. The TPS tower flyby altimeter was found to have not been calibrated during an unknown amount of time prior to the test, and ended up introducing errors into the data. Do not trust that equipment is accurate enough for real world test without calibrating it yourself or confirming calibration methods.

APPENDIX G – DIGITAL DATA

Digital data for this project is organized as follows.

1. Raw Sortie Data

    Flights 1-13
        Balloon Data Folder (when applicable)
        TSPI Data Folder (when applicable)
        Quick-Look Report (Date – Aircrew Names TMP – quicklook.doc)
        DAS Data (Flight X DAS Data.xlsx)
        Filled-In Test Cards (Flight X Test Cards.pdf)

    Ground Cal
        DAS Tail 158 Handheld Ground Cal (DAS Tail 158 Cal.pdf)
        Non-DAS Tail 166 Handheld Ground Cal (NonDAS Tail 166 Cal.xlsx)

    Non Das Flight
        Quick-Look Report
        NonDAS Test Cards

2. Raw MATLAB Imports

    Imported DAS Data, TSPI Data, Balloon Data concatenated into one matrix (FlightX_Date.mat)

3. JMOSS Self Contained Data

    DAS data run through JMOSS without balloon inputs (FlightX_Date_Kt_JMOSS.mat)

4. JMOSS Balloon Temp Data

    DAS data run through JMOSS using balloon temp (FlightX_Date_JMOSS.mat)

5. MATLAB Code
    JMOSS Code (JMOSSV6.m)

6. Miscellaneous

    1 Final Epic Disco GLM.pdf
    2 Initial Epic Disco GLM.pdf
    Figure 14 in 3D (3 GLM Prediction Intervals and TFB Corrections.fig)
    4 C-12 DAS Decoder (C12_DAS_Decoder.xlsx)
    Tower Fly By Data (5 TFB_Data.mat)
    6 TPS Tower Flyby Altimeter Calibration Email.pdf

This page was intentionally left blank.

APPENDIX H – ABBREVIATIONS, ACRONYMS, AND SYMBOLS

Abbreviation	Definition	Units
ADC	air data computer	---
ADS	air data system	---
ADTS	air data test system	---
AFB	Air Force Base	---
AFBI	Air Force Base Instruction	---
AFTC	Air Force Test Center	---
AGL	above ground level	---
ANCOVA	analysis of covariance	---
AOA	angle of attack	degrees
a_{SL}	speed of sound at sea level	knots
ASTM	American Society for Testing and Materials	---
BSEKF	Backwards-Smoothing Extended Kalman Filter	---
CAS	calibrated air speed	knots
CI	confidence interval	---
CG	center of gravity	% MAC
C_L	lift coefficient	---
C_{Lmax}	maximum lift coefficient	---
DISCO	DetermIne Stall Characteristics Online	---
DAS	data acquisition system	---
DSCA	Defense Security Cooperation Agency	---
EPIC	Enhanced Performance Increased Capability	---
F	F-test statistic	---
FAA	Federal Aviation Administration	---
FDR	Flight Data Recorder	---
ft	feet	feet
FTT	Flight Test Techniques	---
g	acceleration of gravity	ft/s^2
GAINR	GPS Aided Inertial Navigation Reference	---
GLM	generalized linear model	---
GPS	global positioning system	---
H_c	truth pressure altitude	feet

$H_{c,tower}$	truth pressure altitude of flyby tower	feet
h_g	geometric altitude	feet
H_i	indicated pressure altitude	feet
H_{ic}	instrument corrected indicated pressure altitude	feet
IAS	indicated airspeed	knots
IMU	inertial measurements unit	---
in. Hg	inches mercury	inches
JMOSS	Jurado-McGehee Online Self Survey	---
JON	job order number	---
K_t	Temperature Correction Factor	---
$\widehat{K}_t$	JMOSS estimated temperature correction factor	---
KCAS	Knots Calibrated Air Speed	---
KIAS	Knots Indicated Air Speed	---
KS	Kolmogorov-Smirnov	---
kts	knots	knots
lb	pound	pounds
M	mach	---
MATLAB	matrix laboratory	---
MSE	mean square error	---
MSL	mean sea level	---
N	sample size	each
n	load factor	---
N/A	not applicable	---
p-value	probability value	---
$\widehat{P}_0$	JMOSS estimated pressure bias	---
P_a	ambient pressure	psi
P_s	static pressure	psi
P_{SL}	sea level static pressure	psi
P_t	total pressure	psi
PA	pressure altitude	---
PFD	Primary Flight Display	---
PPM	precision pressure monitor	---
p	p-value	%
q_c	differential pressure	psi

q_{cic}	instrument-corrected differential pressure	psi
r^2	coefficient of determination	%
RARS	ram air recovery system	---
RPM	revolutions per minute	---
RTB	return to base	---
S	wing planform area	ft^2
SPE	static position error	---
SPEED	static position error enhanced determination	---
SPO	system program office	---
SPSS	Statistical Product and Service Solutions	---
SS	Sum of Squares	---
t	Student's t	---
T_{ic}	instrument corrected temperature	˚C
T_{std}	standard day ambient temperature	˚C
T_{test}	test day ambient temperature	˚C
TFB	tower flyby	each
TGT	turbine gas temperature	˚C
TIM	technical information manual	---
T.O.	technical order	---
TOLD	Takeoff and Landing Data	---
TMP	Test management project	
TP	test plan	---
TPS	Test Pilot School	---
TSPI	time space position information	---
TW	Test Wing	---
USAF	United States Air Force	---
USN	United States Navy	---
$\hat{V}_{W_D}$	JMOSS estimate of Down wind component	ft/s
$\hat{V}_{W_E}$	JMOSS estimate of East wind component	ft/s
$\hat{V}_{W_N}$	JMOSS estimate of North wind component	ft/s
V_c	calibrated airspeed	knots
V_D	GPS down velocity	ft/s
V_e	equivalent airspeed	knots
$V_{e_{stall}}$	equivalent stall airspeed	knots

V_E	GPS East velocity	ft/s
V_e	equivalent airspeed	knots
V_h	maximum level airspeed	knots
V_i	indicated airspeed	knots
V_{ic}	instrument corrected indicated airspeed	knots
V_N	GPS North velocity	ft/s
V_{stall}	stall speed	knots
V_t	true airspeed	knots
W	aircraft gross weight	pounds
W/δ	Weight to pressure ratio	---
WSO	Weapons System Operator	---
Y_i	Sample run	---
$\hat{Y}_i$	Test sample run	---
α	angle of attack	degrees
α_i	indicated angle of attack	degrees
β_i	indicated angle of sideslip	degrees
β	estimated model coefficients	---
δ	pressure ratio	---
ΔH	change in geometric altitude	feet
ΔH_c	change in pressure altitude	feet
ΔH_{ic}	altitude instrument error correction	feet
ΔH_{pc}	altitude position error correction	feet
ΔP_p	static position error	psi
$\Delta \hat{P}_p$	JMOSS static position error estimate	psi
$\Delta P_p / P_s$	static position error ratio	---
ΔV_{ic}	airspeed instrument error correction	knots
ΔV_{pc}	airspeed position correction	knots
η^2	Eta-squared	%
γ	ratio of specific heats	---
γ	flight path angle	degrees
$\mu\Delta\Delta V_{pc}$	mean difference of airspeed position correction	knots
Φ	roll/bank angle	degrees
Ψ	yaw angle	degrees
ρ	density	slugs/ft^3

ρ_{SL}	sea level standard density	slugs/ft^3
Θ	pitch angle	degrees

This page was intentionally left blank.

APPENDIX I – DISTRIBUTION LIST

Onsite	Number of Copies		
	E-mail	Digital	Paper
419 FLTS Attn: Capt John Stevenson 118 E Jones Rd Edwards AFB CA 93524 Email: john.stevenson.10@us.af.mil	1	0	0
Edwards AFB Technical Research Library Attn: Darrell Shiplett 307 E Popson Ave Edwards AFB CA 93524	0	0	2
AFTC/HO Attn: AF Test Center/HO Mailbox 305 E Popson Ave Edwards AFB CA 93524	1	0	0
AFTC/CA Attn: Eileen Bjorkman/Executive Director 1 S Rosamond Blvd Edwards AFB CA 93524 Email: eileen.bjorkman.1@us.af.mil	1	0	0
USAF TPS Attn: Dave Vanhoy 220 Wolfe Ave Edwards AFB CA 93524	1	0	0
USAF TPS Attn: Karl Major 220 Wolfe Ave Edwards AFB CA 93524	1	1	0
USAF TPS Attn: LtCol Juan Jurado 220 Wolfe Ave Edwards AFB CA 93524	1	1	0

Offsite

Defense Technical Information Center Submit per DTIC procedures Attn: DTIC-O 8725 John J. Kingman Rd, Ste 0944 Ft Belvoir VA 22060 Email: aq@dtic.mil	1	0	0
Total	7	2	2